JOURNAL OF MARINE RESEARCH

The *Journal of Marine Research,* one of the oldest journals in American marine science, published important peer-reviewed original research on a broad array of topics in physical, biological, and chemical oceanography vital to the academic oceanographic community in the long and rich tradition of the Sears Foundation for Marine Research at Yale University.

An archive of all issues from 1937 to 2021 (Volume 1–79) are available through EliScholar, a digital platform for scholarly publishing provided by Yale University Library at https://elischolar.library.yale.edu/.

Requests for permission to clear rights for use of this content should be directed to the authors, their estates, or other representatives. The *Journal of Marine Research* has no contact information beyond the affiliations listed in the published articles. We ask that you provide attribution to the *Journal of Marine Research.*

Yale University provides access to these materials for educational and research purposes only. Copyright or other proprietary rights to content contained in this document may be held by individuals or entities other than, or in addition to, Yale University. You are solely responsible for determining the ownership of the copyright, and for obtaining permission for your intended use. Yale University makes no warranty that your distribution, reproduction, or other use of these materials will not infringe the rights of third parties.

Carbon cycling in mesohaline Chesapeake Bay sediments 2: Kinetics of particulate and dissolved organic carbon turnover

by Eric E. Roden[1,2] and Jon H. Tuttle[1]

ABSTRACT

Temporal and depth variations in benthic carbon metabolism rates were examined in relation to particulate organic carbon (POC) deposition rates and particulate and dissolved organic carbon degradation kinetics in two sediments from the mesohaline region of Chesapeake Bay. The depth distribution of a single pool of metabolizable POC (MPOC) in mid-Bay sediments was estimated by curve-fitting of dry weight POC profiles ("1-G" approach). Estimated MPOC pools accounted for 3–4% of total POC content in the upper 10 cm of sediment. First-order MPOC decay constants of ≈ 10 yr^{-1} during the warm season were estimated from the ratio of MPOC pool size to weighted-average MPOC deposition rate derived from mid-water column sediment trap deployments. These results indicated that the MPOC pool defined by the 1-G approach corresponded to the most readily degradable component of coastal marine phytoplankton detritus. Transient-state kinetic models of MPOC turnover, based on observed MPOC deposition rates and temperature-dependent mineralization, predicted MPOC accumulation in sediments during the spring followed by depletion during the summer. The models also predicted an early summer maximum in MPOC mineralization rate associated with the degradation of MPOC accumulated during the spring, in agreement with the seasonal pattern of sulfate reduction rates in mid-Bay sediments. Model results suggested that MPOC deposition during the summer is important in maintaining high rates of benthic carbon metabolism throughout the warm season.

Steady-state and transient-state models of depth-dependent POC degradation suggested that particle mixing influences the depth distribution of MPOC concentration and turnover rate within the upper 4–6 cm of mid-Bay sediments. However, because of the rapid rate of MPOC decay, random particle mixing is unlikely to transport significant quantities of MPOC below 4–6 cm. A steady-state diagenetic model was used to test the hypothesis that downward diffusion of acetate produced by anaerobic decomposition of MPOC in the upper 4–6 cm fuels sulfate reduction deeper in the sediment. The results suggest that because of the very rapid turnover of acetate pools (≥ 2 hr^{-1}), acetate diffusion does not influence the depth distribution of carbon metabolism in the sediment. Therefore, sulfate reduction occurring at depths below 4–6 cm must be fueled by decomposition of some portion of the large pool of relatively refractory sediment POC. Degradation of this material is likely responsible for $\approx 1/3$ of total warm season benthic carbon metabolism.

1. University of Maryland, Center for Environmental and Estuarine Studies, Chesapeake Biological Laboratory, Solomons, Maryland, 20688, U.S.A.
2. Present address: The University of Alabama, Department of Biological Sciences, Box 870206, Tuscaloosa, Alabama, 35487-0206, U.S.A.

1. Introduction

Directly measured or estimated rates of organic carbon (OC) degradation are strongly correlated with long-term rates of sedimentation in marine sediments (Toth and Lerman, 1977; Berner, 1978; Canfield, 1989), presumably due to a global covariation of OC input with sedimentation rate. The gross relationship between OC loading and sediment metabolism has also been established experimentally (e.g. Bågander, 1977; Westrich and Berner, 1984; Kelly and Nixon, 1984; Sampou and Oviatt, 1991). However, the spatial and temporal dynamics of OC degradation in marine sediments can be complex, particularly in shallow-water, temperate coastal regions where rates of OC deposition are high and vary seasonally, and where annual temperature fluctuations are substantial. For example, seasonal variations in the size of sediment organic matter pools have been documented in a few coastal systems (Meyer-Reil, 1983; Rudnick and Oviatt, 1986; Sampou and Oviatt, 1991; Sun *et al.*, 1991), and such changes have been hypothesized to result from a temporal separation of organic deposition and temperature-dependent remineralization (Rudnick and Oviatt, 1986; Kemp, 1988; Klump and Martens, 1989). This effect may accentuate temporal variation in pathways of sediment carbon metabolism, especially in very shallow systems where OC deposition rates are high and anaerobic processes play an important role in sediment metabolism.

Bacterial sulfate reduction (SR) is the principal terminal carbon degradation process in anoxic coastal marine sediments, in which sulfate is typically present at nonlimiting concentrations within the zone of maximal SR activity (Capone and Kiene, 1988). Understanding factors which control rates of SR in coastal sediments is important ecologically, both from the standpoint of carbon and energy flow (Howarth, 1984), and because the reduced S end-products of the process react spontaneously with oxygen and thereby exert a significant impact on oxygen dynamics in shallow coastal waters (Jørgensen, 1977). It has been estimated that SR and oxidation of reduced sulfur compounds account for approximately half of total carbon mineralization and oxygen consumption, respectively, in coastal sediments under waters < 20 m deep (Jørgensen, 1982), and recent studies indicate that S cycling may account for an even greater fraction (up to 80%) of carbon oxidation and sediment oxygen uptake in some shallow water coastal sediments (Mackin and Swider, 1989; Roden *et al.*, 1995). In the mid-Chesapeake Bay, oxidation of reduced S produced in surface sediments may consume a significant amount of oxygen in bottom waters during the late spring/early summer (Roden and Tuttle, 1993; Roden *et al.*, 1995), and water column oxygen consumption coupled to oxidation of H_2S produced in underlying sediments is a major factor maintaining bottom water anoxia during the summer (Tuttle *et al.*, 1987; Kemp *et al.*, 1992; Roden and Tuttle, 1992).

SR rates in coastal marine sediments commonly decrease exponentially with depth as a result of a progressive down-core depletion of labile OC (Berner, 1964; 1980a,b; Jørgensen, 1978b; Berner and Westrich, 1985). This fact and the strong temperature

dependence of sediment SR (e.g., Abdollahi and Nedwell, 1979; Westrich and Berner, 1988) suggest that SR rates in temperate coastal sediments should be maximal when temperatures are relatively warm and an ample supply of reactive OC is present in near-surface sediments. An important question in this regard is the relative importance of freshly deposited, labile OC compared to older, less reactive OC in fueling sediment SR over a seasonal cycle, as this distinction will reflect the extent to which recent organic matter production rates in the water column are linked to SR in the underlying sediments. Recent experimental mesocosm studies have demonstrated that major increases in water column primary production brought on by nutrient enrichment result in increased OC input to sediments and attendant enhancement of sediment SR rates, particularly during the warm season when OC accumulated in surface sediments during the winter/spring is rapidly mineralized (Sampou and Oviatt, 1991). However, the relationship between seasonal patterns of coastal sediment anaerobic metabolism and OC input have not been comprehensively investigated in field-based studies. This task requires complementary information on sediment OC input rate and abundance, as well as information on the rates and kinetics of sediment OC decomposition.

In this paper we present such an examination of OC cycling in mid-Chesapeake Bay sediments by combining recently collected data on particulate organic carbon (POC) deposition, sediment POC content, SR, and ^{14}C-labeled organic substrate metabolism. The present work complements Roden *et al.* (1995) which considers budgetary aspects of OC deposition and sediment OC mineralization in the carbon cycle of mid-Chesapeake Bay. Here we provide an analysis of seasonal variations in OC metabolism through the use of a transient-state kinetic model based on measured rates of POC deposition and estimated first-order MPOC decay constants. We also use the model to illustrate the potential influence of particle mixing on down-core POC diagenesis. In addition, we employ steady-state diagenetic models to examine the possible influence of dissolved OC substrate diffusion on the depth distribution of OC turnover.

2. Materials and methods

a. Station locations and description. The two mesohaline Chesapeake Bay sites (stations R64 and DB) considered here are described in Roden *et al.* (1995). Briefly, station R64 (16 m depth) is located on the western slope of the central channel where overlying waters are hypoxic or anoxic during May–September, whereas station DB (10 m depth) is located on the western flank of the mid-Bay where overlying waters are typically well-oxygenated throughout the year.

b. Sediment POC content. Dry weight POC content was measured in the upper 10 cm of 3–4 sediment cores collected from each of the two mid-Bay stations between March and November, 1986–1988. Subcores (2.5 or 7.6 cm ID) removed from Bouma

Table 1. Parameter values used to estimate the depth distribution and depth-integrated pool size of MPOC (ΣG_m) in mid-Bay sediments.

Station	Depth Interval	[a]G_o (mg C g dry sed^{-1})	[b]G_{nr} (mg C g dry sed^{-1})	α[c] (cm^{-1})	[d]ϕ_0	[d]ϕ_L	β[c] (cm^{-1})	ΣG_m (umol C cm^{-2})
R64	0–4 cm	34.8	23.8	0.764	0.96	0.89	0.463	192
	0–10 cm							207
DB	0–4 cm	32.5	26.4	0.398	0.94	0.83	0.201	229
	0–10 cm							307

[a]Curve-fit value for the dry weight POC concentration at the sediment surface ($x = 0$ cm).
[b]Curve-fit value for dry weight POC concentration at depth (below (5–10 cm) in the sediment, assumed to be nonreactive for purposes of MPOC estimation.
[c]Curve-fit coefficients (see Eqs. 2 and 5 in text).
[d]Curve-fit values for porosity at the sediment surface (ϕ_0) and at depth in the sediment (ϕ_L).

box cores (136 cm^2, ≈ 20 cm deep) were sectioned at 0.5 or 1 cm intervals in the top 2 cm, and at 1–2 cm intervals from 2–10 cm. The sections were frozen immediately at $-20°C$. Thawed sections were weighed before and after drying to a constant weight at 60–100°C (for estimates of sediment porosity) and then pulverized with a mortar and pestle. Subsamples (20–30 mg) were transferred to plastic weigh boats, placed in an acid-fume chamber overnight to remove carbonates, and redried before being weighed out (1–2 mg) for CHN analysis (Control Equipment Co. Model 240XA). Replicate POC determinations from 6–8 cm depth at station R64 had a coefficient of variation of 1.7% ($n = 4$).

The depth distribution and pool size of metabolically labile POC (MPOC) in R64 and DB sediments were estimated by the "1-G" approach (Berner, 1972; Murray et al., 1978; Martens and Klump, 1984). Total dry weight POC (G) approached a constant concentration below depths of 5–10 cm (Fig. 1a,b). This concentration was used as an estimate of the nonreactive fraction of sediment POC (G_{nr}). The difference between total POC concentration and G_{nr} at any given depth x was taken as the MPOC (G_m) concentration; i.e.

$$G_m(x) = G(x) - G_{nr} \tag{1}$$

Eq. 1 assumes that MPOC can be considered a single pool of carbon having uniform reactivity. The dry weight POC profiles were fit by nonlinear least-squares regression to the equation

$$G(x) = (G_o - G_{nr}) \exp(-\alpha x) + G_{nr} \tag{2}$$

where G_o is an estimate of G at the sediment surface ($x = 0$ cm), and α is an

attenuation constant with units cm^{-1} (Table 1). The depth distribution of MPOC is then expressed as

$$G_m(x) = G_m^\circ \exp(-\alpha x) \tag{3}$$

where $G_m^\circ = (G_o - G_{nr})$. Whole sediment MPOC concentration (G_m') (μmol C cm^{-3}) is related to dry weight concentration (mg C g dry sed^{-1}) as follows:

$$G_m'(x) = G_m(x) \cdot [1 - \phi(x)] \cdot 2.6 \cdot (10^3/12) \tag{4}$$

where $\phi(x)$ is sediment porosity at depth x, 2.6 represents the density of dry sediment particles (g cm^{-3}), and the factor $(10^3/12)$ converts from mg C to μmol C units. Measured porosity profiles (data not shown) were fit by nonlinear regression to an equation analogous to (2):

$$\phi(x) = (\phi_0 - \phi_L) \exp(-\beta x) + \phi_L. \tag{5}$$

Depth-integrated pools of MPOC (ΣG_m) were calculated by trapezoidal integration of Eq. 4 over selected depth intervals at 0.5 cm increments.

c. *POC deposition rates.* POC deposition rates were derived from rates of chlorophyll-*a* collection in mid-water column sediment traps (Boynton *et al.*, 1990) as described in Roden *et al.* (1995). We also present here POC collection rates for station R64, along with a summary of the Chl-*a*-derived rates for this location. Deposition data for station DB are presented in Roden *et al.* (1995).

d. *Sulfate reduction.* SR rates were determined using the radiotracer methods of Jørgensen (1978a) as described in Roden *et al.* (1995).

e. *Turnover of ^{14}C-acetate.* Turnover rates of ^{14}C-labeled acetate in intact sediment cores collected during the summer were measured according to Christensen and Blackburn (1982). Either 0.001 or 0.01 μCi of U-^{14}C-acetate (specific activity = 50 mmol mCi^{-1}), was line-injected into 2.5 cm ID subcores at 2 cm intervals from 1 to 9 cm. Injection solutions containing 0.001 and 0.01 μCi ^{14}C had total acetate concentrations of 2 and 20 μM, respectively. Duplicate subcores were incubated at *in situ* temperature (25°C) or at room temperature (22°C) for 5 to 60 minutes (3–4 time points), after which they were sectioned rapidly and bubbled with 10 ml of 4N sulfuric acid to drive off $^{14}CO_2$, which was trapped in a 1:7 mixture of phenethylamine and Instagel (Packard Instruments, Downers Grove, IL) scintillation cocktail. The resulting acid-sediment slurry was centrifuged and radioactivity in the supernatant and CO_2 traps determined by liquid scintillation counting. $^{14}CO_2$ trapping efficiency, determined using NaH$^{14}CO_3$, was 71 ± 8% ($n = 6$). First-order turnover constants for the substrates were determined from semi-log plots of

^{14}C-substrate consumption or ^{14}CO$_2$ evolution as a function of incubation time. Time zero control experiments were used to correct for carryover ($<10\%$ of added radioactivity) of residual ^{14}C-acetate during CO$_2$ trapping.

f. Kinetics of acetate turnover. The rate of ^{14}C-acetate turnover as a function of sediment pore water acetate concentration was examined in station R64 sediments collected from the 0–4 and 12–16 cm depth intervals of box cores. Portions of homogenized sediment (3 ml) were transferred inside an anaerobic chamber to 15 ml serum vials with a 3 ml cutoff syringe. Each portion was amended with 0.3 ml of a sterile, oxygen-free 110 mM Na$_2$SO$_4$ solution to saturate the sediment with sulfate (≥ 10 mmol L^{-1}). The samples were amended with 0.3 ml of a sterile, oxygen-free acetate solution followed 1 min later by addition of 10^5 dpm ^{14}C-acetate, yielding a range of whole sediment acetate concentrations of 5 to 100 μmol L^{-1}. The vial contents were well mixed before and after the addition of ^{14}C-acetate. Duplicate vials were prepared for each concentration level, and duplicate control vials were amended with 0.3 ml of oxygen-free distilled water in place of acetate solution prior to addition of ^{14}C-acetate. Killed controls consisted of sediment treated with 3 ml of 4N HCl prior to addition of ^{14}C-acetate. Incubation times varied from 5 min to 1.5 hr; short incubation times were necessary at low acetate concentrations because of rapid ^{14}C-acetate consumption. Activity was terminated by adding 3 ml of 4N HCl, which volatilized any ^{14}CO$_2$ that formed during incubation. After 2–4 hours equilibration, the headspace of each vial was flushed by N$_2$ stream into a CO$_2$ trap (1:7 phenethyl-amine:Instagel). Each vial was then centrifuged and 1 ml of the supernatant mixed with 5 ml of Instagel. Radioactivity in the supernatant samples and CO$_2$ traps was determined by liquid scintillation counting.

Rate constants for ^{14}C-acetate turnover were plotted against added acetate concentration as described by Li (1983). The data were fit by nonlinear least-squares regression to the function

$$R = \phi V_{max} \cdot [(K + S_n) + \phi C]^{-1}$$

where R is the acetate turnover rate constant (hr^{-1}), V_{max} is the maximum rate of acetate turnover (μmol L^{-1} hr^{-1}), K is the half-saturating acetate concentration for acetate turnover (μM), S_n is the ambient pore water acetate pool size (μM), and C is the whole sediment added acetate concentration (μmol L^{-1}). Both V_{max} and $(K + S_n)$ were allowed to vary during the curve-fitting procedure.

3. Results

a. Sediment POC distributions. Sediment dry weight POC concentrations were highly variable, particularly in the upper 4 cm (Fig. 1a,b). The nonlinear regression fits to these data (solid lines in Fig. 1) must therefore be interpreted as an "average signal" used to make a first approximation of the MPOC content of the sediment. Compa-
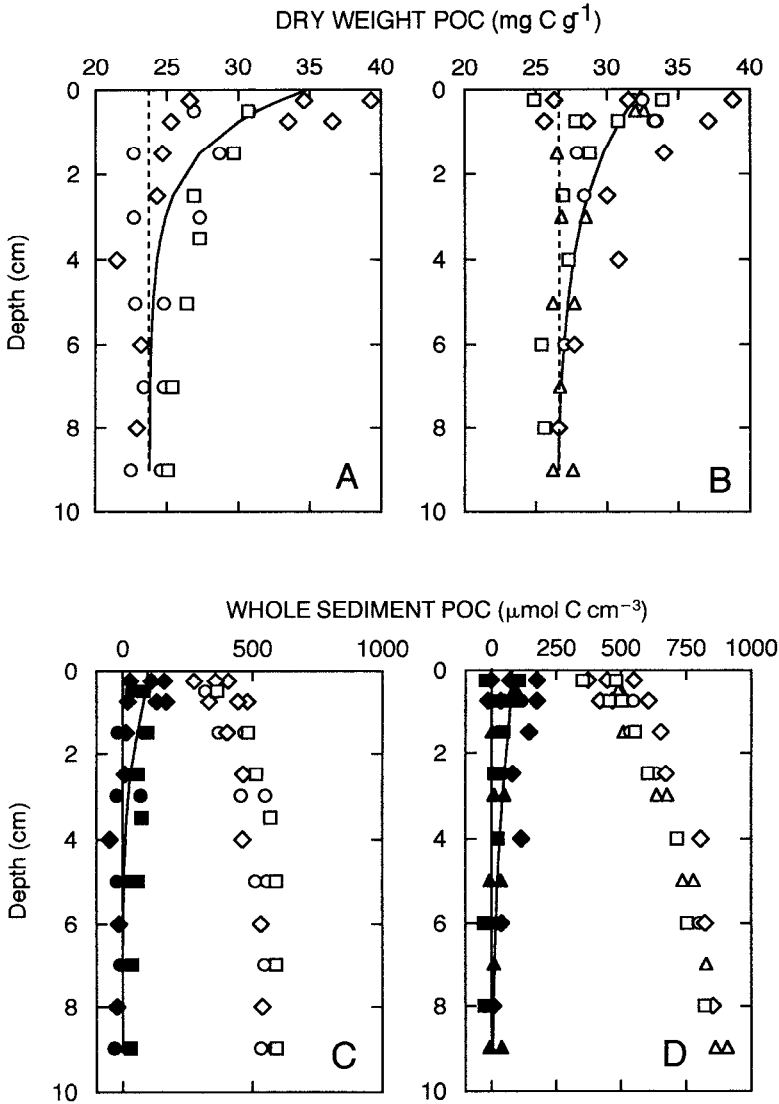
Figure 1. Dry weight POC concentrations measured in R64 (A) and DB (B) sediments, and whole sediment POC (open symbols) and metabolizable POC (MPOC, solid symbols) concentrations calculated from dry weight values using measured sediment porosities for R64 (C) and DB (D) sediments. Samples from station R64 were obtained on 8/14/86 ($\Diamond$), 11/4/87 ($\bigcirc$), and 6/15/88 ($\square$). Samples from station DB were obtained on 3/27/86 ($\Diamond$), 5/14/86 ($\bigcirc$), 8/15/86 ($\square$), and 11/4/87 ($\triangle$). Different symbols represent samples (sometimes taken in duplicate or triplicate) from individual box cores. MPOC was estimated according to Eq. 1 in the text. Solid lines in A and B are nonlinear least squares regression fits, which were combined with porosity distributions to yield the solid lines in C and D (see text). Dashed lines in A and B represent estimates of the nonreactive fraction of sediment POC.

rable levels of variation in sediment POC content have been observed in other coastal sediments (e.g. Martens and Klump, 1984; Berner and Westrich, 1985). Total POC concentrations were large relative to estimated MPOC concentrations, even within the upper few cm of sediment (Fig. 1c,d). The metabolizable fraction of total POC at the sediment surface was 32% at R64 and 19% at DB. MPOC pools integrated over the top 10 cm at R64 and DB (Table 1) corresponded to $\approx 4\%$ of total POC content. The fraction of ΣG_m contained in the top 4 cm was 93% for R64 and 75% for DB (Table 1).

b. POC deposition rates. As noted previously (Roden *et al.*, 1995), POC deposition rates derived from mid-water column sediment trap Chl-*a* collection rates at stations R64 and DB showed a high level of week-to-week variability (averaging $\approx 100\%$ of the weighted-average), but were relatively constant on a time scale of months throughout the warm season (see Fig. 2a, and Fig. 3 in Roden *et al.*, 1995). Total POC deposition rates measured during individual deployment intervals (J_{POC}) were converted to rates of MPOC deposition (J_{MPOC}) for use in kinetic modeling (see below) according to

$$J_{MPOC} = J_{POC} \cdot [(G_{ses} - G_{nr}) \cdot G_{ses}^{-1}] \qquad (6)$$

where G_{ses} is the POC content of suspended seston collected from depths local to where the sediment traps were deployed. This calculation, which is analogous to the 1-G approach used above to estimate sediment MPOC, assumes that seston collected from the water column was representative of the newly produced organic material entering the sediment traps. Also implicit in this calculation of sediment MPOC deposition rate (and the use of sediment trap data in general) are the important related assumptions that (1) the labile organic matter collected in the sediment traps is representative of material which actually reaches the sediment surface (i.e., that this material reaches the sediment surface unaltered relative to its composition in the sediment traps), and (2) that the material collected in the traps is not significantly degraded during the deployment interval. Rigorous analysis of these assumptions is beyond the scope of this paper. The central justification for our use of sediment trap data to constrain rates of MPOC input to mid-Bay sediments for the purpose of the modeling analysis presented below is that, as detailed in Roden *et al.* (1995), the seasonally-integrated POC deposition estimates agree reasonably well with the sum of independently determined sediment metabolism and POC burial rates. Thus, despite the many uncertainties and assumptions involved in the use of sediment traps, they appear to provide a robust estimate of organic carbon input to mid-Bay sediments.

MPOC deposition rates at station R64 derived from mid-water column sediment trap Chl-*a* collection rates are shown in Figure 2a. The daily weighted-average
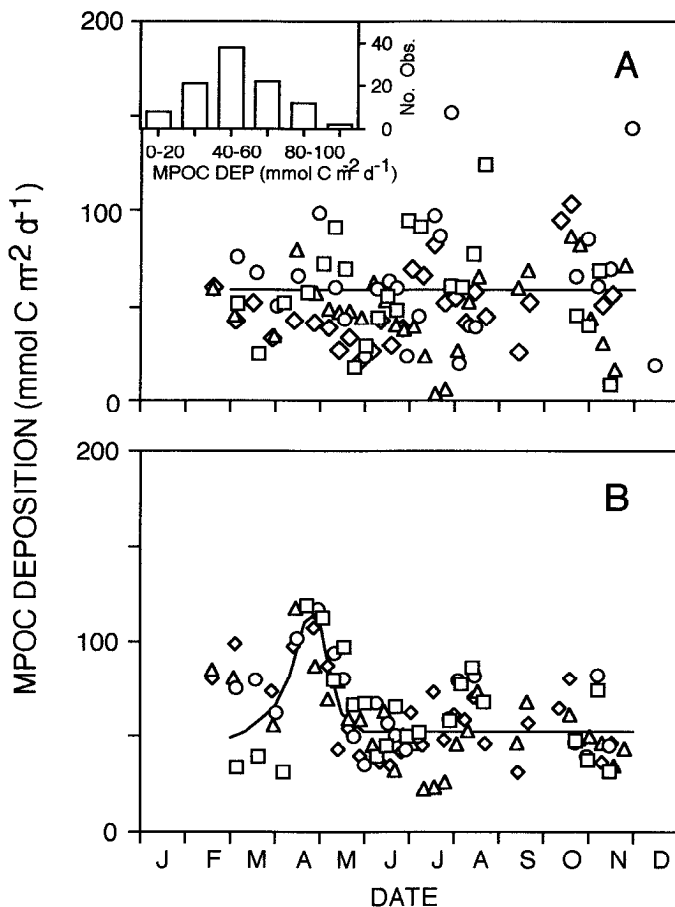
Figure 2. Rates of POC deposition at station R64 derived from rates of Chl-*a* (A) or POC collection (B) in mid-water column sediment traps deployed during 1986 (□), 1987 (○), 1988 (◇), and 1989 (△). The solid line in panel A represents the weighted-average rate for the March–November warm season interval. The solid line in panel B represents a visual (interpolative) fit to the data used for modeling purposes. Inset in panel A shows the frequency distribution of the Chl-*a*-derived MPOC deposition rates.

MPOC deposition rate calculated from these data was 58 mmol C m^{-2} d^{-1}, compared to a weighted-average total POC deposition rate of 65 mmol C m^{-2} d^{-1}. The corresponding Chl-*a*-derived MPOC and total POC deposition rates for station DB were 79 and 115 mmol C m^{-2} d^{-1}, respectively. Estimates of nonreactive POC deposition determined by the difference between total and metabolizable POC input agree well with independent estimates of long-term POC burial based on ^{210}Pb and [239,240]Pu-determined mass sedimentation rates (see Roden *et al.,* 1995).

Whereas Chl-*a*-derived POC deposition rates showed no discernable seasonal pattern, gross POC collection rates in mid-water column sediment traps at station R64 (Fig. 2b) showed evidence of a spring maximum. The observed spring peak in POC collection rate was likely associated with the occurrence and decline of the annual diatom bloom in the mid-Bay. To account for this seasonal pattern in POC deposition for modeling purposes, the data in Figure 2b were fit by visual means (solid lines). Trapezoidal integration of the area under the solid line in Figure 2b yielded a weighted-average MPOC deposition rate (75 mmol C $m^{-2} d^{-1}$) comparable to the weighted-average Chl-*a*-derived rate.

c. Sulfate reduction rates. Areal SR rates in mid-Bay sediments undergo a strong seasonal variation (Roden and Tuttle, 1993; Roden *et al.*, 1995). SR data for stations R64 and DB are reproduced here (Figs. 3 and 4) to illustrate that maximum SR rates tend to occur during the early summer, rather than during August when mid-Bay bottom water temperatures reach their annual maximum. Additional measurements made at station R64 in years subsequent to 1989 (Marvin, 1995) have confirmed this phenomenon. Summer SR rates were maximal in the upper few cm of R64 and DB sediments and decreased exponentially with depth (Fig. 5).

d. Turnover of ^{14}C-acetate. Rate constants for ^{14}C-acetate uptake and respiration ranged from 1 to 10 times hr^{-1} in the upper 10 cm of R64 and DB sediments during the summer (Table 2). Rate constants determined using a tracer solution with a total (labeled plus unlabeled) acetate concentration of 2 µM were 2–3 times higher than those determined with 20 µM acetate solution (Table 2). Acetate turnover kinetics experiments in homogenized R64 sediment (Fig. 6) gave estimates of 2–6 µM for the parameter $(K + S_n)$.

4. Discussion

a. Acetate pool size and turnover kinetics. Acetate turnover rates measured in mid-Bay sediments were comparable to those determined in other coastal marine sediments (Ansbaek and Blackburn, 1980; Balba and Nedwell, 1982; Christensen and Black-burn, 1982; Sansone and Martens, 1982; Shaw *et al.*, 1984; Novelli *et al.*, 1988; Michelson *et al.*, 1989; Shaw and McIntosh, 1990). We combined ^{14}C-acetate turnover rates with SR rates determined in parallel cores to estimate concentrations of microbially available acetate (MAA) according to the equation (Novelli *et al.*, 1988)

$$C_x = (\phi_x \cdot R_x \cdot f)u_x^{-1} \qquad (7)$$

where C_x is the porewater MAA concentration (µM), ϕ_x is sediment porosity, R_x is the SR rate (µmol $L^{-1} hr^{-1}$), f is the fraction of SR fueled by acetate metabolism, and u_x is the acetate turnover constant (hr^{-1}) at depth x. This approach assumes that SR

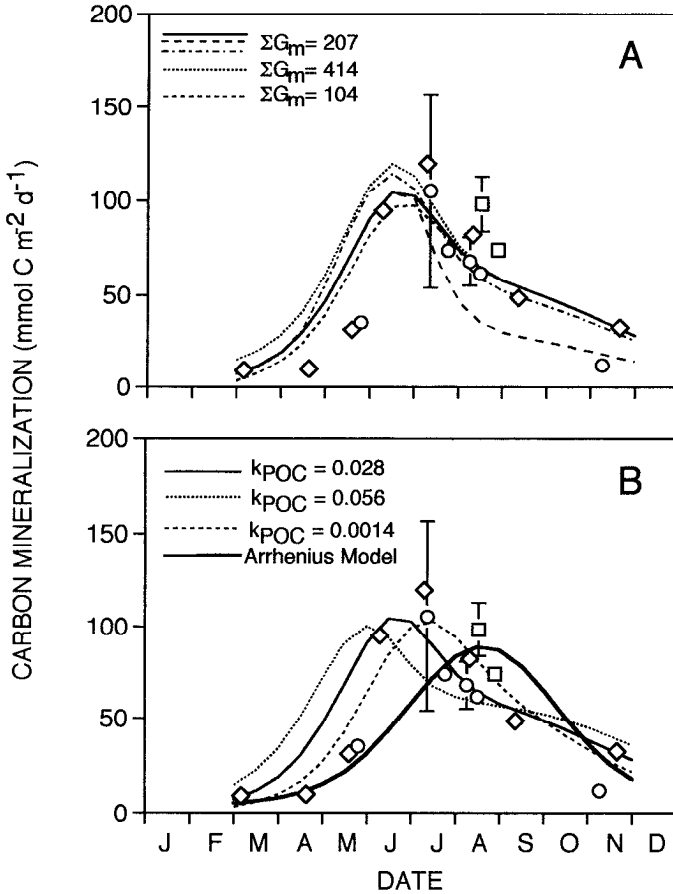Figure 3. Mean areal SR rates for station R64 (open symbols; error bars indicate ±1 SD, $n = 2$–6) expressed in carbon equivalents ($1S = 2C$), and rates of carbon mineralization predicted by a transient state kinetic model (lines). SR data are from 1986 ($\square$) and 1987 ($\bigcirc$) and 1989 ($\Diamond$). 1989 rates are the unpubl data of M. Marvin and D. Capone. Solid lines indicate transient-state kinetic model simulations made using the depth-integrated (0–10 cm) MPOC estimates (ΣG_m) listed in Table 1 as the initial ($t = 0$, julian date 60) MPOC pool sizes, and the reference POC decay constants (k_{POC}) and weighted-average MPOC deposition rates (J_{MPOC}) listed in Table 3. Dotted and short dashed lines indicate simulations made using different initial ΣG_m and reference k_{POC} values. The long dashed line in panel A indicates a simulation made using standard ΣG_m and k_{POC} values, but employing a two-fold decrease in the MPOC deposition rate after 1 July. The dot-dash-dot line in panel A indicates a simulation using standard ΣG_m and k_{POC} values, but employing a time-varying POC deposition rate as described by the solid line in Figure 2b. Arrhenius model predictions in panel B refer to those made by combining fits of measured areal SR rates to the Arrhenius equation with a time/temperature function for each station as described in Roden and Tuttle (1993).
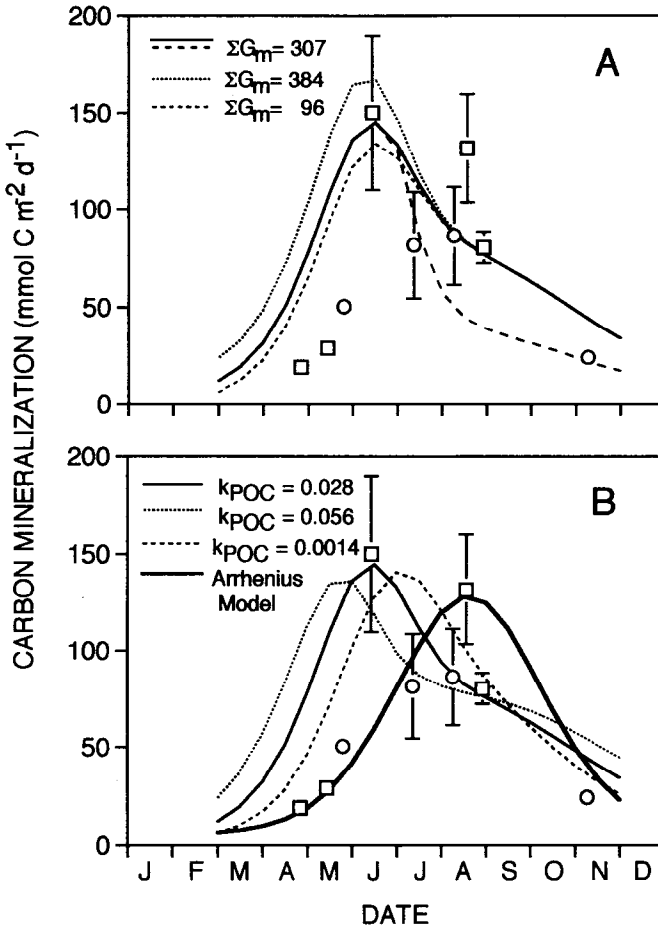
Figure 4. Mean areal SR rates for station DB (open symbols; error bars indicate ± 1 SD, n = 2–6) expressed in carbon equivalents (1S = 2C), and rates of carbon mineralization predicted by a transient state POC kinetic model (lines; see Fig. 3 legend). SR data are from 1986 (□) ànd 1987 (○).

was the dominant acetate mineralization process in anoxic mid-Bay sediments, which is reasonable given that other electron acceptors (e.g. NO_3^-, metal oxides) are not abundant in mid-Bay sediments, and that nonlimiting concentrations of sulfate are present within the upper 10 cm of these sediments (Roden and Tuttle, 1993). We chose a value of 0.6 for f, based on the findings of Sørensen *et al.* (1981), Winfrey and Ward (1983), Christensen (1984), Parkes *et al.* (1989), and Shaw and McIntosh (1990). Estimated MAA concentrations fell in the range of 1–10 μM (data not shown), in agreement with estimates for other coastal marine sediments (Christensen and Blackburn, 1982; Shaw *et al.*, 1984; Novelli *et al.*, 1988; Shaw and McIntosh, 1990).

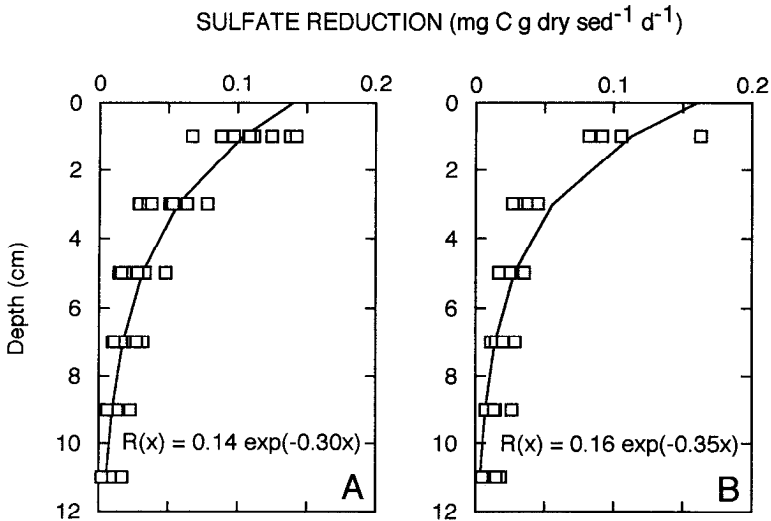SULFATE REDUCTION (mg C g dry sed^{-1} d^{-1})

Figure 5. Depth profiles of SR rate measured during the summer at stations R64 (A) and DB (B). Measured porosity distributions (Table 1) were used to convert whole sediment SR rates to a dry weight basis. Each data point represent the average of 2–6 determinations made on parallel cores on a given sampling date. Solid lines represent curve fits of the data to the equation $R(x) = R_o \exp(-Zx)$, where R_o is the SR at the sediment surface ($x = 0$), and Z is an attenuation constant.

The predicted range of MAA concentrations was consistent with the results of turnover experiments conducted with tracer solutions having 10-fold different total acetate concentrations. ^{14}C-acetate uptake and respiration constants determined using 2 µM acetate were 2–3 times higher than those determined with 20 µM acetate (Table 2). Analogous results have been reported by Ansbaek and Blackburn (1980) and Balba and Nedwell (1982). Dilution of the ambient acetate pool with labeled and unlabeled acetate in the vicinity of the line of tracer injection was probably responsible for this effect. That a modest but distinct dilution effect was observed with tracer solutions of 2–20 µM suggests that ambient MAA concentrations were within this range.

Because sediment homogenization and addition of sulfate may have altered rates of acetate metabolism in mid-Bay sediments, the results of our acetate turnover kinetics experiments (Fig. 6) should be interpreted with caution. It is significant to note, however, that the estimated $(K + S_n)$ values for acetate turnover (2–6 µM) are consistent with the range of MAA concentrations predicted on the basis of measurements made in undisturbed sediment cores. In addition, our $(K + S_n)$ values agree with those estimated for freshwater sediments in which SR was the dominant terminal carbon mineralization process (Lovley and Klug, 1983), and with steady-state acetate concentrations in such sediments (Lovley and Phillips, 1987). To our knowledge, these measurements represent the first such determination of kinetic

Table 2. First-order ^{14}C-acetate uptake and respiration rate constants measured in sediments at station R64 (August 1987) and DB (July 1987). Triplicate (R64) or duplicate (DB) cores were incubated for 5, 10 and 15 minutes for each rate constant determination.

Station	Series[a]	Depth Interval (cm)	Uptake Constant[b] (hr^{-1})	Respiration Constant[c] (hr^{-1})
R64	A	0–2	6.9 ± 1.3	6.3 ± 1.0
		2–4	7.4 ± 1.0	4.4 ± 1.3
		4–6	5.3 ± 1.3	4.9 ± 1.0
		6–8	5.9 ± 0.8	4.3 ± 0.7
		8–10	6.4 ± 0.6	2.9 ± 0.7
			Mean: 6.4 ± 0.8	Mean: 4.6 ± 1.2
R64	B	0–2	3.7 ± 1.8	2.5 ± 1.3
		2–4	2.1 ± 0.5	1.1 ± 0.4
		4–6	1.9 ± 0.5	1.5 ± 0.4
		6–8	2.1 ± 0.5	1.1 ± 0.2
		8–10	1.9 ± 0.1	1.0 ± 0.2
			Mean: 2.3 ± 0.8	Mean: 1.4 ± 0.6
DB	B	0–2	2.1 ± 0.2	
		2–4	2.0 ± 0.3	
		4–6	2.7 ± 0.1	
		6–8	2.5 ± 0.1	
		8–10	2.9 ± 0.4	
			Mean: 2.4 ± 0.4	

[a]Series A and B cores were injected with tracer solutions having total acetate concentrations of 2 μM (3.0×10^3 dpm/injection) and 20 μM acetate (2.7×10^4 dpm/injection), respectively.

[b]Calculated from the slope of semilog plots of % ^{14}C-acetate activity remaining in sediment pore fluid versus incubation time; error represents the standard error of the slope.

[c]Calculated from the slope of semilog plots of $[A/(A - a)]$ versus incubation time, where A = dpm ^{14}C-acetate injected, and a = dpm [14]CO_2 recovered at time t; error represents standard error of the slope.

parameters for acetate turnover in coastal marine sediments. Perhaps the most important outcome of these experiments is the exponential decrease in ^{14}C-acetate turnover rate constant observed with increasing acetate pool size (Fig. 6), which clearly demonstrates how a slight elevation of ambient substrate concentration during introduction of tracer solutions can significantly lower the measured rate constant.

The above and numerous other estimates of coastal marine sediment porewater MAA concentrations are significantly lower than total acetate concentrations typically measured in such sediments, owing to the fact that a major portion of the acetate pool in coastal sediments is apparently present in a pool which is biologically unavailable on time scales (a few minutes to a few hours) typical of ^{14}C-acetate turnover experiments (Christensen and Blackburn, 1982; Parkes *et al.*, 1984; Gibson *et al.*, 1989; Wellsbury and Parkes, 1995). Because of this phenomenon, the use of ^{14}C tracers to estimate absolute rates of carbon flow in anaerobic coastal sediments is
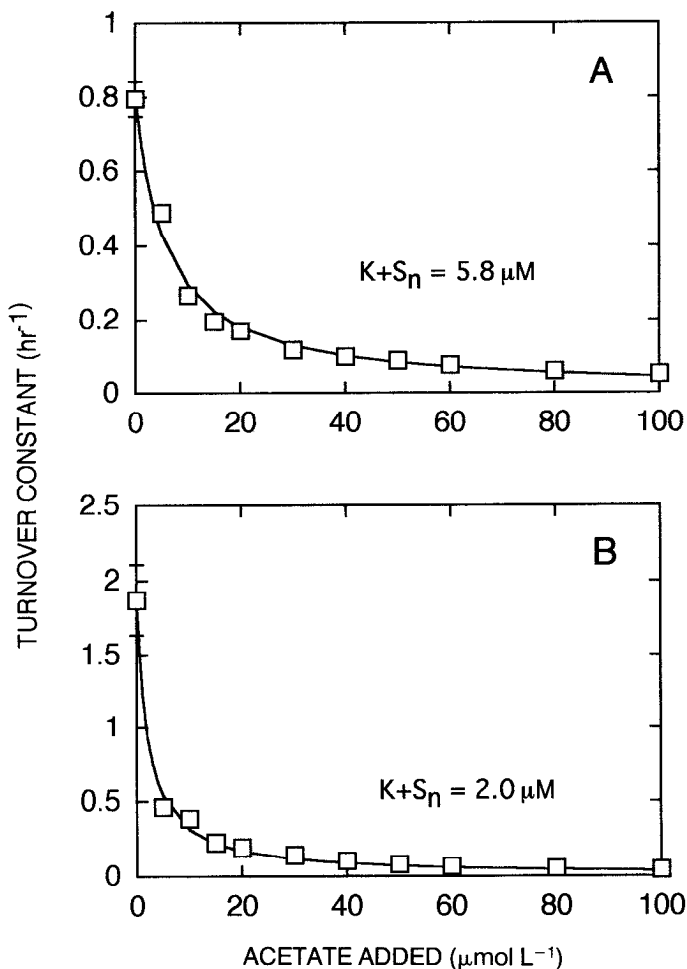
Figure 6. Variation of ^{14}C-acetate turnover rate with addition of unlabeled acetate. Error bars indicate the range of duplicate samples. Nonlinear least squares regression fits (solid lines) were used to estimate the kinetic parameter $(K + S_n)$, equal to the sum of the half-saturation constant (K) and the ambient, microbially available acetate pool size (S_n) (see text). Panels A and B show results for the 0–4 and 12–16 cm sediment depth intervals, respectively, at station R64. Experiments were conducted with homogenized sediment from each depth interval.

problematic. Rather, studies of ^{14}C-labeled substrate metabolism are useful mainly in assessing the distribution and turnover kinetics of dissolved substrates fueling SR in coastal marine sediments. We provide an example of one such approach later in this paper in the course of assessing controls on the depth distribution of carbon mineralization in mid Chesapeake Bay sediments.

Table 3. First-order MPOC decay constants (k_{POC}, k_{SR}) calculated from depth-integrated MPOC pool sizes (ΣG_m) and March–November weighted-average rates of MPOC deposition (J_{MPOC}) and depth-integrated summer SR rates (ΣSR) at stations R64 and DB.

Station	Depth Interval	ΣG_m (μmol C cm^{-2})	J_{MPOC} (μmol C cm^{-2} day^{-1})	k_{POC} (day^{-1})[a]	k_{POC} (yr^{-1})[b]	ΣSR (μmol C cm^{-2} day^{-1})	k_{SR} (day^{-1})[c]	k_{SR} (yr^{-1})[d]
R64	0–10 cm	207	5.82	0.028	10.3	7.47	0.036	13.2
DB	0–10 cm	307	7.90	0.025	9.4	8.17	0.027	9.7

[a]$k_{POC} = (J_{MPOC} \times \Sigma G_m^{-1})$.
[b]$k_{POC} = (J_{MPOC} \times \Sigma G_m^{-1}) \times 365$.
[c]$k_{SR} = (\Sigma SR \times \Sigma G_m^{-1})$.
[d]$k_{SR} = (\Sigma SR \times \Sigma G_m^{-1}) \times 365$.

b. Kinetics of MPOC turnover in mid-Bay sediments. Below we compare rates of MPOC deposition and mineralization with estimated MPOC pool sizes to calculate first-order MPOC decay constants, which are later used to construct a kinetic model of MPOC turnover in mid-Bay sediments. Inherent in these comparisons is the assumption that our MPOC pool size (ΣG_m) estimates are valid as first approximations. We also note that although the MPOC pool size estimates are derived from pooled measurements made on several occasions at each station, they do not represent weighted-average values analogous to those available for POC deposition. Thus, the MPOC decay constants derived from these estimates must also be regarded as first-approximations, useful mainly for constructing the kinetic model. Two justifications for this approach (see below) are: (1) the calculated POC decay constants are comparable to those determined experimentally in marine sediments; and (2) the model predicts seasonal trends in MPOC abundance and turnover rate which are relatively insensitive to the particular MPOC values chosen.

First-order decay constants (k_{POC} values) for MPOC were calculated from the ratio of weighted-average MPOC deposition rate to total MPOC pool size in the upper 10 cm of sediment. These values are compared with decay constants (k_{SR} values) calculated from the ratio of the average summer areal SR rate (in carbon equivalents) to ΣG_m in Table 3. The latter calculations were made on the assumption that all MPOC turnover was coupled to SR during the summer. This seems reasonable in light of arguments presented elsewhere (Roden and Tuttle, 1993). MPOC decay constants based on MPOC deposition rates were comparable to those based on summer SR rates (Table 3). That the latter values were slightly higher is not surprising considering that they are based on SR rates occurring at peak summer temperatures. The decay constants based on MPOC deposition rates were assumed to correspond to a temperature of 17°C, the weighted-average temperature during the March–November time period over which the deposition data were integrated.

The *k* values listed in Table 3 are similar in magnitude to initial rates of fresh

plankton degradation via SR in anaerobic marine sediments at 20–22°C (Westrich and Berner, 1984). Thus, our estimates of MPOC appear to represent "G_1" material (Westrich and Berner, 1984), i.e., relatively fresh, highly labile OC, representing ≈ 50 of the total POC content and $\approx 70\%$ of the metabolizable POC content of fresh plankton. Approximately 20% of fresh plankton POC (referred to as "G_2" material by Westrich and Berner, 1984) decays anaerobically at 10-fold lower rate than the G_1 fraction, whereas about 30% of plankton carbon is essentially nonmetabolizable (or is transformed into a nonmetabolizable form) on a time scale of years. The latter percentage is in approximate agreement with the difference between annual POC deposition rates and annual rates of permanent POC burial in the mid-Bay, which suggests that 20–30% of deposited POC is nonmetabolizable (Roden *et al.*, 1995). The relative importance of G_1 and G_2 material in fueling SR in mid-Bay sediments is discussed below.

Our first-order MPOC decay constant estimates agree within a factor of 2–3 with those determined for Cape Lookout Bight, NC sediments by a POC depth distribution curve-fitting procedure (Martens and Klump, 1984, and with those determined experimentally in surface (0–2 cm) southern Chesapeake Bay (Burdige, 1991) and near-surface (2–6 cm) Long Island Sound sediments (Westrich and Berner, 1984). Burdige (1991) found that estimated POC decay constants decreased with depth in the upper 15 cm of sediment, and suggested that the POC being degraded in surface sediments was predominantly G_1 material, whereas the POC being degraded further down in the sediment was representative of G_2 or an even more refractory G_3-type material. This assertion agrees with our finding that most of the MPOC in mid-Bay sediments is contained within the top 4 cm, and with our contention that this MPOC is representative of G_1 material.

c. Modeling seasonal variation of MPOC pool size and turnover rate. The MPOC decay constants listed in Table 3 correspond to turnover times of 1–2 months for the sedimentary MPOC pool. Because these residence times are significantly shorter than seasonal cycles (e.g. of temperature, POC production/deposition) in the mid-Bay, the possibility exists for major seasonal variations in the sediment MPOC pool size and turnover rate (Martin and Bender, 1988). Specifically, these MPOC residence times suggest that (1) accumulation of MPOC in mid-Bay surface sediments during spring (at relatively cold temperatures) could be important in fueling rates of sediment metabolism during the onset of the warm season, and that (2) POC deposited during the summer may be important in maintaining rates of sediment metabolism throughout the latter part of warm season. A transient-state kinetic model was used to examine these hypotheses quantitatively.

In its simplest form, the model ignored the depth distribution of MPOC, i.e. ΣG_m was treated as single sedimentary pool. The ΣG_m estimates derived from POC profiles (Table 1) were used as initial values, and MPOC pool size changes were

predicted on the basis of a March–November weighted-average rate MPOC deposi-
tion rate (J_{MPOC}) and temperature-dependent first-order MPOC decay, i.e.

$$d\Sigma G_m(t)/dt = J_{MPOC} - k_{POC}(T(t)) \cdot \Sigma G_m(t) \qquad (8)$$

where $k_{POC}(T(t))$ is the first-order MPOC decay constant at temperature T and time t
(julian date). The Arrhenius equation was used to describe the temperature depen-
dence of the decay constant, assuming an apparent activation energy (E_a) of 83 kJ
mol^{-1}. This value, which corresponds to a Q_{10} of 3.5 between 5 and 25°C, was chosen
based on the results of fits of R64 and DB areal SR rates to the Arrhenius equation
(Roden and Tuttle, 1993) and is comparable to others published values of the
temperature dependence of SR in coastal sediments (Westrich and Berner, 1988).
Reference values for k_{POC} were defined by the ratio of MPOC deposition rate to
MPOC pool size (k_{POC} in Table 3). These k values were assumed to correspond to the
weighted-average temperature during the March–November time period (17°C) over
which the modeling was conducted. Temperature variations were described by a
sinusoidal function fit to bottom water temperature data for each station (see Roden
and Tuttle, 1993). Eq. 8 was solved numerically at daily time increments ($dt = 1$)
according to the expression

$$\Sigma G_m(t+1) = \Sigma G_m(t) + [d\Sigma G_m(t)/dt] \cdot dt \qquad (9)$$

from julian date 60 to 330 (March through November).

The model predicted a substantial seasonal change in the pool size of MPOC
(Fig. 7, solid line). A two-fold increase was predicted from March through May,
followed by a rapid decrease during the summer. Minimum MPOC pool sizes were
predicted during the late summer. Predicted rates of MPOC turnover were maximal
in early summer (Figs. 3 and 4, solid lines), about 1.5 months after the peak in MPOC
accumulation. This pattern differs from that yielded by the Arrhenius model used
previously to describe the seasonal variation of SR rates in mid-Bay sediments
(Roden and Tuttle, 1993), in which predicted POC degradation rates (shown in
Figs. 3 and 4 for comparison) follow the annual temperature cycle and are therefore
maximal in the late summer.

The sensitivity of the model to changes in parameter values was tested by varying
individually the initial MPOC pool size and reference decay constant values by a
factor of two and re-running the models (using the weighted-average MPOC input
rates). We note here that changing the MPOC deposition rate led to proportional
changes in the magnitude of predicted MPOC pool sizes and turnover rates, but did
not affect the timing of their maxima and minima (data not shown). Increasing or
decreasing the value of the initial MPOC pool size did not change the overall
seasonal variation of MPOC pool size and turnover rate, and the timing of the peak
spring accumulation of MPOC and the early summer turnover rate maximum were
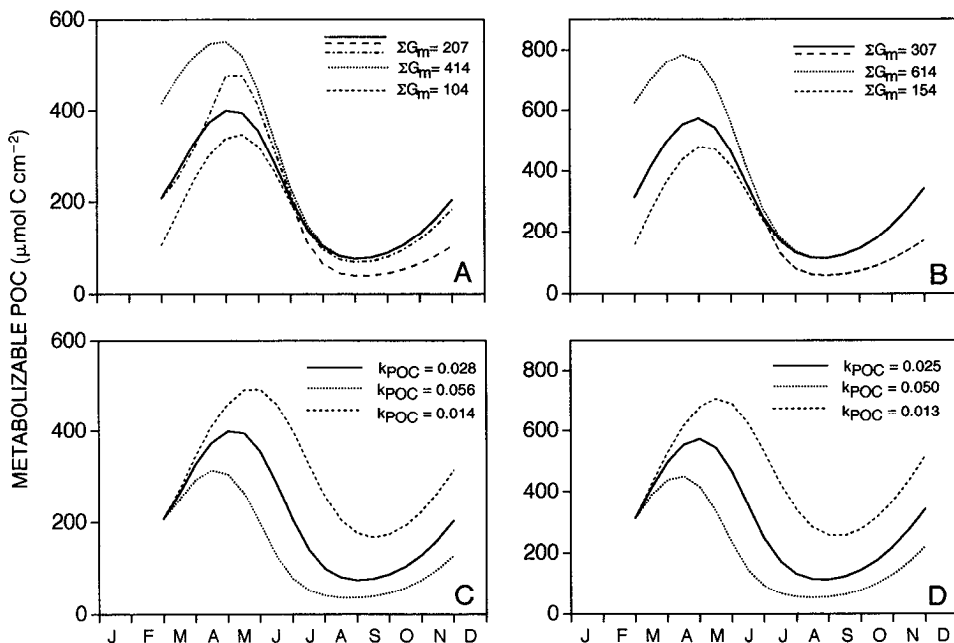
Figure 7. Variation of MPOC pool size in R64 (A, C) and DB (B, D) sediments predicted by a transient-state kinetic model. Solid lines indicate model simulations made using the depth-integrated (0–10 cm) MPOC estimates (ΣG_m) listed in Table 1 as the initial ($t = 0$, julian date 60) MPOC pool sizes, and the reference POC decay constants (k_{POC}) and weighted-average MPOC deposition rates (J_{MPOC}) listed in Table 3. Dotted and short dashed lines indicate simulations made using different initial ΣG_m and k_{POC} values. Long dashed lines in panels A and B indicate simulations made using standard ΣG_m and k_{POC} values, but employing a two-fold decrease in the MPOC deposition rate after 1 July. The dot-dash-dot line in panel A indicates a simulation using standard ΣG_m and k_{POC} values, but employing a time-varying POC deposition rate as described by the solid line in Figure 2b.

offset by only ≈ 10 days (Figs. 3a and 4a). Predicted MPOC pool sizes converged to similar value after ≈ 90 days.

When the reference POC constant was varied by a factor of two, the timing of the peak spring accumulation of MPOC and the early summer MPOC turnover rate maximum were significantly affected (Figs. 3b and 4b). Nevertheless, the model still predicted a spring accumulation of MPOC followed by a rapid consumption of this material associated with an early summer maximum in MPOC degradation. Because March–November integrated estimates of MPOC deposition (upon which the models are based) and carbon flow through SR agree within 20–30% (Roden *et al.*, 1995), the predicted rates of carbon turnover approximate the direct measurements. More importantly, the models consistently predicted an early summer maximum in MPOC turnover, which agreed with early summer SR rate maxima observed at both stations.

In order to assess how a variable MPOC deposition rate, in particular one accounting for a spring maximum associated with the annual diatom bloom, would affect model predictions, the MPOC deposition rates derived from mid-water column POC collection rates (Fig. 2b) were used as input to the model. These data were used because no coherent seasonal variation in POC deposition rate could be discerned from the Chl-a-derived deposition rates. The corresponding time-integrated rate of MPOC deposition (defined by the area under the solid line in Fig. 2b) differed by $\approx 30\%$ from that defined by the weighted-average POC deposition rate (area under the solid line in Fig. 2a). For consistency, the same reference MPOC decay constant was used. Thus, the primary difference between these two model runs was the seasonal pattern of MPOC input. The spring accumulation of MPOC predicted by the model employing a spring maximum in MPOC input rate was higher than that predicted by the model employing a constant MPOC input rate (Fig. 7a), although the difference in MPOC accumulation was only $\approx 20\%$. Accordingly, rates of MPOC turnover in the late spring/early summer predicted by the former model were higher by a comparable margin (Fig. 3a). These results confirm the logical expectation that a spring maximum is POC deposition will enhance the spring accumulation of POC in surface sediments, which will translate into an enhanced peak in sediment carbon metabolism later in the season.

To evaluate the sensitivity of model predictions to random variations in MPOC deposition rates, which are clearly suggested by the high variability observed in both Chl-a and POC collection rates (Fig. 2), the model was run using a randomly-varying MPOC input rate produced by a random number-generating algorithm. This algorithm (which incorporated the random number generator included in the Turbo Basic programming language in which the program was written) generated random numbers between 0 and 1 according to a normal distribution with a mean of zero and a standard deviation of 1 (Press *et al.*, 1992). The algorithm was used to choose (at varying time steps) MPOC deposition rates at random from a normal distribution with mean and standard deviation equal to that calculated for the Chl-a-derived POC deposition data by using the expression:

$$J_{MPOC} = J_{MPOCmean} + (\text{random number}) \cdot J_{MPOCsdev} \qquad (10)$$

where $J_{MPOCmean}$ and $J_{MPOCsdev}$ are the mean and standard deviation of the Chl-a-derived MPOC deposition rates shown in Figure 2a (equal to 54.3 and 26.2 mmol C m^{-2} d^{-1}, respectively.) New deposition rates were chosen in this manner every 1, 3, 6, or 15 days over the 270 day simulation period in order to simulate random variations in deposition occurring over different characteristic time scales, i.e. daily, a few days, one week, and two weeks. In each case, the model was run five times, using a different "seed" value to start the random number generator on the first day of the simulation. The variability in MPOC pool size and turnover rate among the five model runs increased substantially as the time interval over which each randomly chosen deposition rate was applied increased from 1 to 15 days (Fig. 8). This
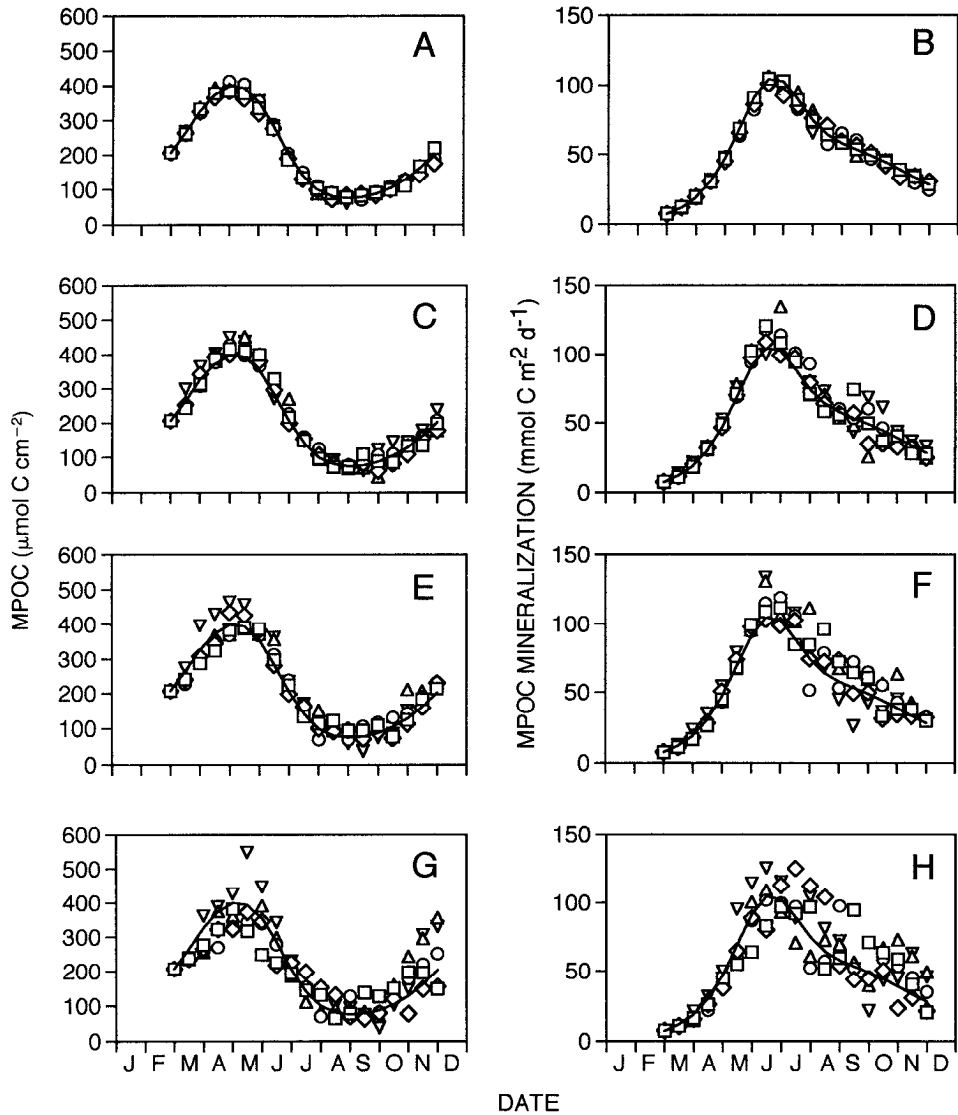
Figure 8. Variation of MPOC pool size (left-hand panels) and mineralization rate (right-hand panels) in R64 sediments predicted by transient-state models employing a randomly-varying MPOC deposition rate (see text). Results in panels A & B, C & D, E & F, and G & H represent simulations in which a new deposition rate was randomly-selected every 1, 3, 6, or 15 days, respectively. In each case, the model was run 5 times (different symbols in each panel), using a different "seed" value to start the random number generator on the first day of the simulation. All simulations were made using the ΣG_m values listed in Table 1 as the initial (julian date 60) MPOC pool size, and the reference k_{POC} values listed in Table 3.

variability was accentuated in the latter part of the simulation period, presumably due to the cumulative effect of variations in MPOC input over the preceding months. However, the seasonal variations in MPOC pool size and mineralization rate predicted by the constant-input model were preserved. These results together with the other model sensitivity analyses presented above show that although variations in parameters associated with MPOC turnover in mid-Bay sediments may influence the exact timing and magnitude of seasonal fluctuations in MPOC pool size and turnover rate, the predicted pattern of spring MPOC accumulation and an early summer MPOC turnover rate maxima associated with the degradation of this accumulated carbon was consistent and repeatable in all cases.

Model-predicted rates of MPOC turnover during the spring were several-fold higher than measured rates of SR, which suggests that other carbon mineralization pathways (e.g., aerobic respiration) were important during the spring. If we assume a 1:1 ratio of oxygen consumption to aerobic carbon respiration (Jørgensen, 1977), Spring rates of sediment oxygen consumption at stations R64 and DB (20–30 and 40–50 mmol m^{-2} d^{-1}, respectively; Roden *et al.*, 1993) are comparable to predicted rates of springtime MPOC turnover. It seems reasonable that aerobic carbon oxidation could have been the dominant source of sediment oxygen demand during the spring, when rates of SR are relatively low and therefore oxygen consumption linked to sulfide oxidation was probably minimal. The fact that predicted MPOC turnover rates agree well with sediment oxygen consumption rates in the spring and SR rates in the summer and autumn indicates that the kinetic model yields a realistic picture of the seasonal variation of carbon mineralization rates in mid-Bay sediments. Our model results support the idea that a major shift from aerobic to anaerobic sediment carbon mineralization pathways occurs during the late spring/ early summer, which is suggested by the seasonal variation of the ratio of sediment oxygen consumption to SR in mid-Bay sediments (Roden *et al.*, 1995). This shift appears to be accentuated by the onset, during late spring/early summer, of degradation which had accumulated earlier in the season when temperatures were much lower.

The quantity of MPOC predicted to accumulate during the spring (weighted-average MPOC input model with standard ΣG_m and k_{POC} parameter values) was compared with total MPOC deposition to assess the quantitative significance of this phenomenon. This accumulation, 2.1 and 2.6 mmol C m^{-2} from julian date 60–120 (March–April) at stations R64 and DB, respectively, equaled $\approx 50\%$ of total MPOC deposition at both stations during this time interval. Changes in POC abundance of this magnitude represent a relatively small signal ($< 20\%$) compared to the total pool of POC in the upper 4 cm of mid-Bay sediments, which explains why attempts to detect systematic temporal changes in mid-Bay surface sediment POC abundance have been unsuccessful (P. A. Sampou, pers. comm.). The above estimates of MPOC accumulation are sufficient to fuel ≈ 1 month of summer SR at the average rates

(80–100 mmol C m^{-2} d^{-1}) determined for stations R64 and DB. Given that SR occurs at rates comparable to summer averages for at least 3 months (June–August; Fig. 2), these results suggest that summertime MPOC deposition must be important in maintaining high summer rates of SR in mid-Bay sediments. To evaluate this, the POC kinetic models were run using standard parameters, except that the weighted-average MPOC deposition rate for each station was decreased by one-half after julian date 180 (1 July). Toward the end of the summer, predicted MPOC pool sizes and turnover rates were ≈2-fold lower than those predicted assuming a constant J_{MPOC} (Fig. 2a,b and 5a,b dotted lines). The latter rates were 2–4 times lower than measured rates of carbon flow through SR. The results suggest that a major portion of warm season sediment carbon metabolism is fueled by deposition during the summer (see further discussion of this point below). Primary production in the mid-Bay region is maximal during the summer (Sellner, 1987; Malone *et al.*, 1988), and deposition of a substantial fraction of this production is suggested by differences between gross primary production and net water column respiration rates (Boynton *et al.*, 1990).

Our kinetic model results are consistent with other studies documenting seasonal variations of organic matter abundance in coastal sediments. Rudnick and Oviatt (1986) estimated an accumulation of 1.25 mol C m^{-2} during winter/spring in MERL mesocosms, equal to ≈50% of total POC sedimentation during that period. Other experiments in MERL mesocosms have demonstrated higher levels of spring POC build-up (≈ 4 mol C m^{-2} in nonnutrient enriched systems; Sampou and Oviatt, 1991). During summer and autumn, progressive depletion of accumulated POC, which could be accounted for by measured rates of carbon mineralization, was observed such that little or no net accumulation of organic material occurred (Sampou and Oviatt, 1991). This finding is consistent with that of Rudnick and Oviatt (1986) in that the magnitude of winter/spring sediment POC accumulation was similar to the deficit between benthic carbon mineralization and gross carbon sedimentation during the summer (Doering *et al.*, 1986). In an examination of Chl-*a* diagenesis in Long Island Sound sediments, Sun *et al.* (1991) found maximum sediment Chl-*a* inventories in April and May and minimum inventories during late summer. Similar variations in the abundance of Chl-*a* have been reported for Buzzards Bay (Massachusetts) sediments (Banta *et al.*, 1995), and the decay of labile OC deposited during the spring bloom has been suggested as an explanation for late spring maxima in sediment oxygen consumption observed in these sediments. Together these studies point to positive net ecosystem production and associated storage of organic matter in sediments as a common feature of shallow-water temperate coastal ecosystems. In systems with well-developed benthic macrofaunal communities, such accumulations of sedimentary organic matter may constitute a crucial food supply for the aerobic benthic food chain during the summer (Rudnick and Oviatt, 1986). In contrast, in the mid-Chesapeake Bay sediments examined in this study such accumulations appear to

set the stage for the onset of high rates of SR and associated sulfide oxidation, i.e. a predominance of anaerobic metabolic pathways.

d. Depth distribution of MPOC concentration and mineralization: influence of particle mixing. Our curve-fit estimates of the ratio of MPOC to total POC content in surface (0–2 cm) mid-Bay sediments (10–30%) are comparable to those estimated by a similar procedure for Cape Lookout Bight, NC sediments (Martens and Klump, 1984). These ratios are also comparable to those determined experimentally for Long Island Sound (Westrich and Berner, 1984) and southern Chesapeake Bay (Burdige, 1991) sediments. The agreement of curve-fit versus experimentally determined MPOC abundances suggests that the former procedure yields a reasonable estimate of the abundance of G_1-type material in superficial coastal marine sediments.

The depth distribution of SR rate in mid-Bay sediments (Fig. 3) qualitatively resembled that of sediment POC content (Fig. 1a,b). At both stations, SR rates decreased much more rapidly with depth above the 4 cm horizon than below it. This decrease paralleled a rapid decline in estimated MPOC concentration within this interval (Fig. 1c,d), suggesting that G_m (i.e. "G_1") material fuels SR in the upper 4 cm of mid-Bay sediments. We emphasize the qualitative nature of this comparison, given the high degree of variability in both SR rate and sediment POC concentration measurements, and the fact that these measurements were not all made on the same cores. However, modeling results presented below provide independent support for the contention that G_m material is important in fueling SR in the upper 4 cm of mid-Bay sediments.

Berner and Westrich (1985) observed that sediment POC concentration decreased far less with depth than that predicted by estimation of the total amount of carbon flow through SR that occurred during accumulation of the sediment layer in question. We found similar results when these calculations were applied to mid-Bay sediments (data not shown). Berner and Westrich (1985) interpreted their results as evidence of down-mixing of newly deposited POC. Below we pursue a further analysis of the influence of particle mixing on sediment POC diagenesis by addressing two questions: (1) does inclusion of particle mixing in steady-state diagenetic models improve estimation of first-order MPOC decay constants from depth profiles of POC content and SR rate (relative to those estimated assuming no particle mixing), and (2) what, if any, influence may particle mixing have on temporal changes in the depth distribution of MPOC in mid-Bay sediments? Our overall goal was to assess qualitatively the potential influence of particle mixing on SR beneath the sediment surface.

A one-dimensional general diagenetic equation for MPOC undergoing burial, random particle mixing, and first-order decomposition is (Berner, 1980a)

$$\delta G'_m/\delta t = \delta[D_m(\delta G'_m/\delta x)]/\delta x - \omega \delta G'_m/\delta x - kG'_m \tag{11}$$

where G'_m is in units μmol C cm^{-3} whole sediment, D_m is the particle mixing coefficient (cm^2 yr^{-1}), ω is the sediment burial rate (cm yr^{-1}), and k is the first-order decay constant (yr^{-1}). By assuming steady-state conditions ($\delta G'_m/\delta t = 0$), an average sediment porosity, an average sediment burial rate (ω = constant), and no particle mixing, Eq. 11 simplifies to

$$\omega\delta G_m/\delta x - kG_m = 0. \tag{12}$$

The solution to this equation, with a constant surface concentration ($x = 0, G_m = G^\circ_m$) as the boundary condition, is

$$G_m = G^\circ_m \exp\left[(-k/\omega)x\right]. \tag{13}$$

The parameter α in the dry weight POC curve fit equations (Table 1) can be identified with (k/ω), yielding ($\alpha\omega$) as an estimate of k (Berner, 1980a). If we assume that SR mediates all G_m mineralization (a first approximation only, although as discussed below this is almost certainly the case during the period of peak sediment metabolism in the summer), then SR rate profile curve fits (Fig. 3) can also be used to estimate k (Berner, 1980a). The k values and MPOC turnover rates estimated using Eq. 13 (Table 4, $D_m = 0$) are an order of magnitude lower than those derived from estimates of G_m deposition and mineralization (Table 3). This nonconcurrence demonstrates that consideration of sediment burial and first-order decay alone does not produce an accurate model of *in situ* MPOC turnover.

   Random particle mixing coefficient estimates for mid-Bay sediments (Table 4) are in the high range of those estimated for nearshore marine sediments (Matisoff, 1982). Activities of a *Nereis/Macoma* macrofaunal community (Holland, 1988) are probably responsible for particle mixing at station DB. During the spring, mid-Bay channel sediments are also colonized by *Macoma* and *Nereis,* as well as smaller polychaetes (Spionidae) (Holland, 1988; Kemp *et al.,* 1990). These organisms probably cause particle mixing in the upper few cm of R64 sediment during the spring, but the disappearance of this community during anoxia/hypoxia precludes bioturbation as a particle mixing process during the summer.

   Berner and Westrich (1985), examining sediments similar to those of the mid-Bay central channel, concluded that some mechanism(s) other than sediment burial was involved in carbon input to near-surface sediments underlying anoxic/hypoxic bottom water during the summer. They suggested that gas bubble ebullition, driven by methane production beneath the SR zone, provided an additional source of metabolizable carbon input to the near-surface SR zone. We propose an alternative interpretation, namely that the passage of gas bubbles upward through the sediment-water interface causes particle mixing, which transports newly deposited MPOC downward into the upper several cm of sediment. Although this explanation is speculative, observations of bubble ebullition in mid-Bay central channel cores brought from depth to atmospheric pressure aboard ship clearly indicated the

Table 4. First-order MPOC decay constants (k) derived from POC (Fig. 1a,b) and SR rate (Fig. 4) profiles.

Station	ω[a] (cm yr^{-1})	D_m[b] (cm^{-2} yr^{-1})	Profile	Attenuation[c] Coefficient (cm^{-1})	k[d] (yr^{-1})	MPOC[e] Turnover (mol m^{-2} yr^{-1})
R64	0.625	0	POC	0.764	0.478	0.99
	0.625	0	SR	0.300	0.188	0.44
	0.625	10	POC	0.764	6.31	13.07
	0.625	10	SR	0.300	1.09	2.26
DB	0.962	0	POC	0.398	0.380	1.17
	0.962	0	SR	0.350	0.337	1.03
	0.962	25	POC	0.398	4.34	13.32
	0.962	25	SR	0.350	3.40	10.44

[a]Average sediment burial rate in the corresponding depth interval, calculated from

$$\omega = \omega_{dm} \times [(1 - \phi_{avg}) \cdot 2.6]^{-1}$$

where ω_{dm} is the annual dry mass sedimentation rate (g cm^{-2} yr^{-1}, see Roden *et al.*, 1995), ϕ_{avg} is the average porosity in the corresponding depth interval (0.92 for R64, 0.88 for DB), and 2.6 is the density of dry sediment particles (g cm^{-3}).

[b]Particle mixing coefficient; the value of 10 cm^{-2} yr^{-1} for R64 was estimated from [7]Be distributions measured at a nearby 15 m channel slope location (D. L. Rice, pers. comm.); the value of 25 cm^{-2} yr^{-1} for DB is that estimated from ^{210}Pb distributions at a nearby 15 m western flank location (Officer *et al.*, 1984).

[c]Values are taken from Table 1 (POC profiles) and Figure 4 (SR rate profiles).

[d]Estimated by identifying POC and SR rate profile attenuation coefficients with theoretical diagenetic expressions (Berner, 1980a). Details of the calculations are given in the text.

[e]Calculated as $k\Sigma G_m$. ΣG_m values are those listed in Table 1.

possibility of particle mixing during bubble transport. Of course, the intensity of *in situ* ebullition must be less than that observed at atmospheric pressure. However, that methane ebullition does in fact occur in mid-Bay sediments can be inferred from depth distributions of the inert gases argon and nitrogen (Reeburgh, 1969), quantitative consideration of pore water sulfide diagenesis (Roden and Tuttle, 1992), and from sonar scan observations of gas bubbles in mid-Bay bottom waters during summer anoxia/hypoxia (S. Brandt, unpubl data). Thus, it is not unreasonable to postulate that this process could cause particle mixing in mid-Bay channel sediments, especially during the summer when sulfate is depleted rapidly with depth and methane reaches saturating or near-saturating concentrations at depth in the sediment (Roden and Tuttle, 1992; Marvin, 1995).

Although rates of particle mixing may vary seasonally and with depth in mid-Bay sediments, the mixing coefficients listed in Table 4 were assumed to be time- and depth-independent for the purpose of making a first assessment of the role of particle mixing in sediment carbon diagenesis. A random particle mixing coefficient was included in the steady-state diagenetic equation for MPOC (Eq. 11) assuming

the following boundary conditions: (1) $x = 0$, $G_m = G_m^\circ$, and (2) $x \to \infty$, $G_m \to 0$. With these boundary conditions (assuming an average porosity and sedimentation rate; Table 4), the solution to Eq. 11 is

$$G_m = G_m^\circ \exp\{[\omega - (\omega^2 + 4kD_m)^{1/2}]/2D_m\}x \qquad (14)$$

By identifying α from the POC profile curve fits (Fig. 1) and Z from the SR rate profile curve fits (Fig. 3) with the expression

$$\{[\omega - (\omega^2 + 4kD_m)^{1/2}]/2D_m\} \qquad (15)$$

we determined an additional set of k values for each station (Table 4). These estimates, invoking particle mixing, are closer to those based on direct measurements of MPOC deposition and mineralization (Table 3) than those based on Eq. 13. Although the agreement between k values estimated from Eq. 13 and those based on direct carbon flux measurements does not allow us to causally infer down-mixing of MPOC, the results are consistent with the hypothesis that particle mixing influences POC diagenesis in mid-Bay surface sediments.

Transient-state solutions to Eq. 11 were made with and without inclusion of a particle mixing term to test more directly the potential influence of particle mixing on POC diagenesis. The numerical approach of Peng and Broecker (1979) was employed, with the following specifications: (1) a sediment layer of thickness L was divided into L 1 cm sublayers ($dx = 1$); (2) mixing within each sublayer was assumed to be instantaneous; (3) the surface layer received a constant input of MPOC (J_{MPOC}); (4) the particle mixing rate was time- and depth-independent; (5) the dry mass sedimentation rate (g cm^{-2} yr^{-1}) was time-independent, but the linear sedimentation rate (cm yr^{-1}) varied with depth according to down-core porosity change (see Table 1); (6) the MPOC decay constant varied with temperature according to the Arrhenius equation ($E_a = 20$ kcal mol^{-1}).

The rate of change in whole sediment MPOC concentration in each sublayer was calculated by the following equations:

$$dG_m'(1)/dt = D_m[G_m'(2) - G_m'(1)]/dx^2$$
$$- \omega(1)G_m'(1)/dx + J_{MPOC} - k_{POC}G_m'(1) \qquad (16)$$

$$dG_m'(i)/dt = D_m[G_m'(i-1) - 2G_m'(i) + G_m'(i+1)]/dx^2$$
$$+ \omega(i)[G_m'(i-1) - G_m'(i)]/dx - k_{POC}G_m'(i) \qquad (17)$$

$$dG_m'(L)/dt = D_m[G_m'(L-1) - G_m'(L)]/dx^2$$
$$+ \omega(L)[G_m'(L-1) - G_m'(L)]/dx - k_{POC}G_m'(L). \qquad (18)$$

The model was iterated from julian date 60 (1 Mar) to 330 (30 Nov) at 1 day time increments. Initial depth distributions of whole sediment MPOC concentration were
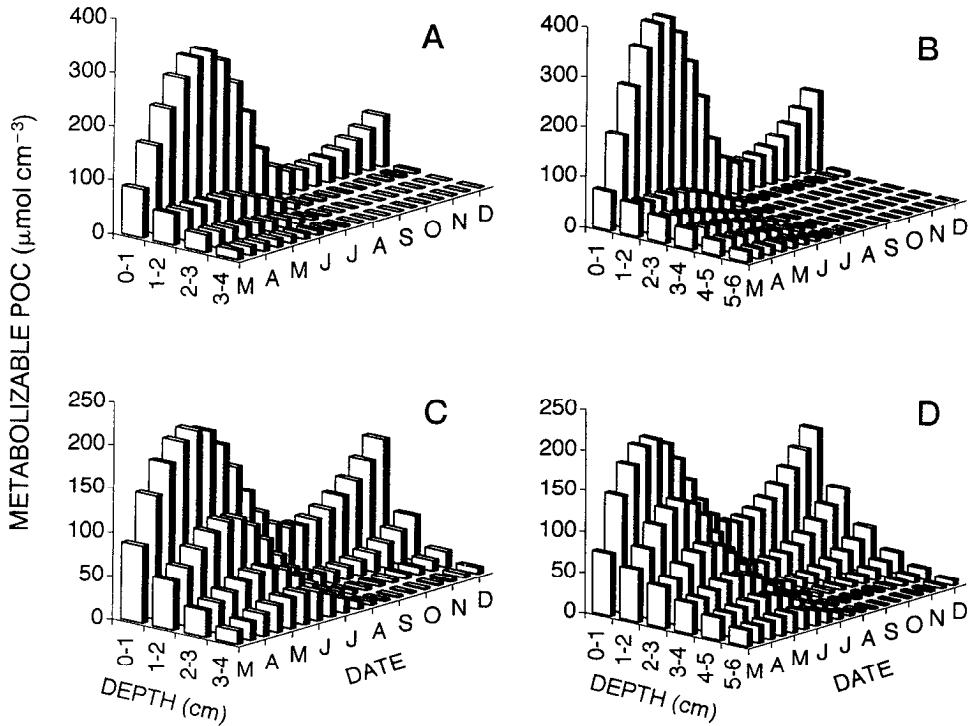
Figure 9. Model predictions of temporal and down-core variations of MPOC concentration in R64 (A, C) and DB (B, D) sediments. A and B: model ignored particle mixing ($D_m = 0$). C and D: model included random particle mixing ($D_m = 10$ and 25 cm^2 yr^{-1} for R64 and DB, respectively). The model employed the weighted-average MPOC deposition (J_{MPOC}) and reference k_{POC} values listed in Table 3 to predict MPOC depth distributions over time according to Eqs. 14–16 in the text. Initial MOPC depth distributions were those described by the solid lines in Figure 1c,d.

those estimated from measured POC profiles (Fig. 1c,d, solid lines). The J_{MPOC} and k_{POC} values (Table 3) were those used in the transient-state model described previously (Eq. 7). Only the upper 4 cm were considered in the model for station R64, because 4 cm approximates the mixed layer depth discerned from ^{210}Pb profiles (Dibb and Rice, 1989) and very little of the estimated MPOC pool at R64 was present below 4 cm (Fig. 1c). Although the top 10 cm of sediment was included in the model for DB sediments, predicted changes in MPOC content were trivial below 6 cm. Model runs for each station used the D_m values given in Table 4, or used $D_m = 0$ for no particle mixing.

When particle mixing was ignored, most of the deposited MPOC accumulated in the surface layer (Fig. 9a,b). Below this layer, $G_m(x)$ was lower than the initial value at all $t > 0$. Seasonal oscillations in G_m occurred only in the top 2 cm, and increases in $G_m(x)$ over initial values occurred only in the top 1 cm. At linear sedimentation rates

on the order of 1 cm yr^{-1} at both stations (Table 4), and warm season k values of 5–10 yr^{-1} (Table 3), most MPOC reaching the sediments would be expected to be mineralized within the top 1 cm in the absence of particle mixing. Accordingly, nearly all of predicted MPOC turnover occurred in the top layer (data not shown). This prediction is inconsistent with SR rate profiles, which indicated a more equitable distribution of SR reduction activity over the upper 4 cm (Fig. 3).

Inclusion of particle mixing in the models caused increased MPOC concentrations (Fig. 9c,d) and turnover rates (not shown) at depth in the sediment. Even so, very little newly deposited MPOC penetrated deeper than 4 cm. This agrees with the rapid decline in estimated MPOC concentrations within this depth interval at both stations (Fig. 1c,d). Similar conclusions were reached by Westrich and Berner (1984) regarding the fate of "G_1" material reaching coastal marine sediments in which nonadvective particle transport can be treated as a random mixing process. The reason for this is that fresh MPOC is almost entirely decomposed before particle mixing can transport it below the upper few cm. Random particle mixing rates much higher than those estimated for mid-Bay sediments would be required to transport freshly deposited POC to depths approaching 10 cm. This strongly suggests that the MPOC (as defined by our estimation procedure) is mineralized mostly within the upper 4 cm of sediment at both stations. Thus, particle mixing acts mainly to distribute newly deposited MPOC within this interval.

The significant rates of SR (Fig. 3) and ^{14}C-acetate turnover (Table 2) observed below 4 cm depth in mid-Bay sediments could be explained by slow turnover of some portion of the large pool of (presumably relatively refractory) POC at depth in the sediment, or by downward diffusion of labile dissolved OC (produced by the breakdown of the MPOC pool in the upper 4 cm) fueling anaerobic metabolism further down in the sediment. The first hypothesis is reasonable, given that $\approx 30\%$ of the metabolizable fraction of fresh plankton (G_2 material) decays at a rate about 10 times slower than the rest (Westrich and Berner, 1984). Because of the large and variable background concentration of POC at depth in mid-Bay sediments (Fig. 1), we cannot make reasonable estimates of the G_2 pool of less reactive POC. Thus, we can only suggest that if decay of G_2 material fuels SR below 4 cm, it is responsible for $\approx 30\%$ of total SR occurring in the upper 10 cm of sediment.

The second hypothesis to explain substantial SR below 4 cm in mid-Bay sediments requires rapid downward diffusion of metabolizable dissolved OC. Acetate diffusion has been suggested as a mechanism by which labile OC in the upper few cm of sediment can reach the anaerobic microbial community deeper in the sediment (Michelson *et al.*, 1989; Shaw and McIntosh, 1990). We examined this hypothesis by a steady-state modeling approach similar to that of Novelli *et al.* (1988).

e. Diagenetic models of acetate turnover. We used a one-dimensional equation describing a steady-state balance between diffusion, production, and first-order consump-

tion of microbially available acetate (MAA)

$$D_s \delta^2 C(x)/\delta x^2 + R(x) = uC(x) \tag{19}$$

where $C(x)$ represents whole sediment MAA concentration (μmol cm^{-3}), D_s is the sediment diffusion coefficient for acetate (cm^2 d^{-1}), $R(x)$ is the acetate production rate (μmol cm^{-3} d^{-1}), and u is the first-order consumption rate constant (d^{-1}). For simplicity, we used a depth-averaged rate constant, which is not unrealistic given the similarity of ^{14}C-acetate turnover constants determined in the upper 10 cm of mid-Bay sediments (Table 2). Two models were developed: Model 1 was based on acetate production defined by first-order decay of MPOC, whereas Model 2 was based on an acetate production rates derived from measured SR rates. In the former model, the MPOC decay constants used were those determined from the ratio of depth-integrated summer SR rate to MPOC pool size (k_{SR} in Table 3), which assumes implicitly that *all MPOC turnover was mediated by SR during the summer.* This assumption is almost certainly valid for channel station R64 where bottom waters are hypoxic or anoxic throughout the summer. Based on estimates of SR and sulfide oxidation versus rates of sediment oxygen consumption, this assumption is probably reasonable for station DB as well (Roden and Tuttle, 1993).

Parameter values and descriptions for Models 1 and 2 are presented in Table 5. Eq. 19 was integrated numerically by a nonlinear finite difference algorithm (Burden *et al.*, 1981). A numerical approach was used so that the influence of porosity variation on the depth distribution of whole sediment MPOC concentration could be taken into account (Table 5). We chose boundary conditions:

$$x = 0, C = C_o \text{ and } x \to \infty, C \to 0$$

The second boundary condition was approximated by setting $C = 0$ at a depth of 20 cm. The use of lower boundary depths (> 20 cm) did not influence model predictions.

The key assumption which permitted testing of the diffusion hypothesis by modeling was that depth-integrated MPOC turnover and carbon flow through SR in the top 10 cm were equal during the summer. If the diffusion hypothesis is correct, depth profiles of MAA concentration and turnover rate predicted on the basis of MPOC decay (Model 1) should be similar to those predicted on the basis of SR rates (Model 2) throughout the upper 10 cm of sediment, despite the fact that most MPOC was located in the upper 4 cm (Fig. 1c,d).

For brevity, we present only the model results for station R64 since those for station DB showed very similar patterns. MAA concentration and turnover rate profiles predicted by Model 1, like estimated distributions of MPOC concentration and turnover rate, showed distinct maxima in the upper few cm of sediment, as well as a rapid decrease with depth below these maxima (solid lines in Fig. 10a,d). In

Table 5. Parameters used in steady-state models of MAA turnover.

| | Model 1[a] | | | | Model 2[b] | | | | | |
| | G_m° | | | | R_0 | | | D_s^c | C_o^d | u^e |
Sta.	(mg C g^{-1})	α (cm^{-1})	k (d^{-1})	f	(mg C g^{-1} d^{-1})	Z (cm^{-1})	f	(cm^2 d^{-1})	(umol cm^{-3})	(d^{-1})
R64	11.0	0.764	0.036	0.6	0.140	0.300	0.6	0.93	0.002	154
DB	6.1	0.398	0.027	0.6	0.160	0.350	0.6	0.85	0.002	167

[a]Acetate production was defined by $R(x) = 0.5 f k_{SR} G_m^\circ \exp(-\alpha x) [1 - \phi(x)](2.6)(10^3/12)$. The factor 0.5 accounts for the fact that acetate contains two equivalents of reduced carbon. k_{SR} is the first order decay constant for metabolizable POC calculated on the basis of the estimated standing stock of metabolizable POC and the average summer areal sulfate reduction rate in the upper 10 cm (Table 3). Values for G_m° and α are from curve fits to profiles of dry weight POC (mg C g dry sed^{-1}) content (Fig. 1; Table 1).

[b]Acetate production was defined by $R(x) = 0.5 f R_0 \exp(-Zx) [1 - \phi(x)](2.6)(10^3/12)$. R_0 and Z were defined by nonlinear regression analysis of measured sulfate reduction rate profiles (Fig. 5). The factor 0.5 accounts for the fact that acetate contains two equivalents of reduced carbon. The parameter f accounts for the assumption that 60% of sulfate reduction is fueled by acetate turnover. The porosity distributions ($\phi(x)$) are those given in Table 1. A value of 2.6 was assumed for the density of dry sediment particles. The factor $(10^3/12)$ converts from units of mg C to umol C.

[c]D_s = sediment diffusion coefficient for acetate, derived from the free solution value (D_o) of 1.12 cm^2 d^{-1} (Michelson et al., 1989) according to

$$D_s = \phi_{avg}^2 \times D_o$$

where ϕ_{avg} = average sediment porosity in the upper 10 cm of sediment. This formula provides an approximate correction for sediment tortuosity (Berner, 1980a).

[d]C_o = concentration of acetate at the sediment water interface ($x = 0$). C_o was estimated from measured sulfate reduction and ^{14}C-acetate uptake rates in anoxic mid-Bay bottom waters (J. Tuttle, unpubl data).

[e]u = average acetate uptake constant in the to 10 cm of intact sediment cores (see Table 2); a 2 μM (2.7 $\times$ 10^{3}dpm per injection) ^{14}C-acetate tracer solution was employed for station R64 sediments (August 1987); a 20 μM (2.7 $\times$ 10^4 dpm per injection) ^{14}C-acetate tracer solution was employed for station DB sediments (July 1987), and the measured average uptake rate constant (60 d^{-1}) was corrected for dilution of the sediment acetate pool during injection of 20 μM tracer solution based on relative rates of ^{14}C-acetate uptake in R64 cores injected with 2 vs. 20 μM tracer solutions.

contrast, smaller near surface peaks and a more gradual down-core decline of MAA concentration and turnover rate were predicted by Model 2 (solid lines in Fig. 10b,e).

MAA profiles back-calculated from SR and MPOC turnover rate distributions using Eq. 7 and depth-averaged u values (Fig. 10a,b, symbols) were identical to those predicted by the models using the D_s values listed in Table 5 (Fig. 10a,b, solid lines), i.e. consideration of diffusion did not alter predicted MAA distributions (except in the top few mm where the profiles were constrained by the upper boundary
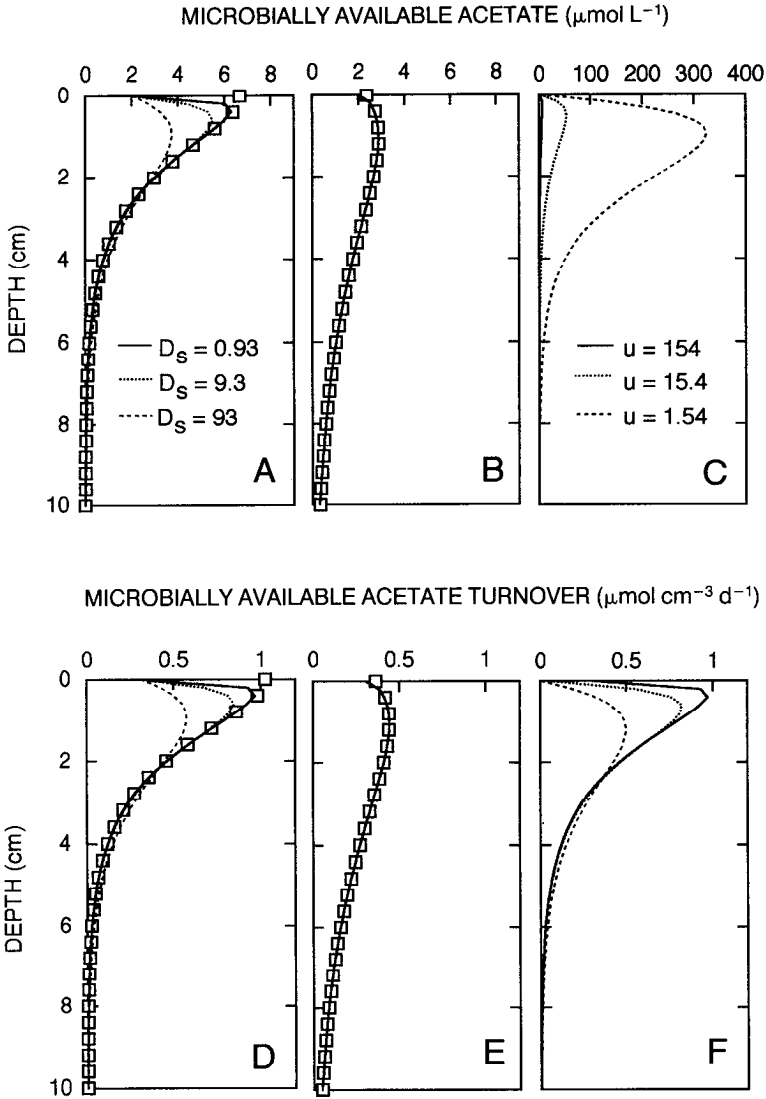
Figure 10. Steady-state model predictions of MAA concentrations (A, B, C) and turnover rates (D, E, F) in R64 sediments during the summer. The rate of MAA turnover at each depth was calculated as the product of the predicted MAA concentration and the depth-averaged first-order MAA uptake constant. Panels A and D: Model 1 (see text and Table 5) results. In panel A, model predictions (lines) made with a range of sediment diffusion coefficient (D_s) values are compared with estimates (symbols) back-calculated (Eq. 7 in the text) from the ratio of MAA production rate to decay constant at each depth. Symbols in panel D represent the MAA production function upon which the model was based. Panels B and E: Model 2 (see text and Table 5) results. In panel B, model predictions (solid line) are compared with estimates (symbols) back-calculated from the ratio of MAA production rate to decay constant. Symbols in panel E represent the MAA production function upon which the model was based. Panels C and F: Model 1 predictions made with a range of MAA uptake constants (u).

concentration of 2 μmol L^{-1}. We attribute this agreement to the extremely rapid turnover of MAA pools: MAA produced by OC decay in the upper few cm of sediment would have little chance of diffusing downward before being consumed by sulfate-reducing bacteria. To examine this idea, we decreased the value of the acetate turnover constant (u) by a factor of 10 or 100. This led to a substantial increase in MAA concentrations (in proportion to the change in u) and deeper penetration of MAA downward into the sediment (Fig. 10c). However, because of the lower turnover rate constants, predicted MAA oxidation rates at depth in the sediment did not increase (Fig. 10f). Interestingly, decreasing u resulted in a major increase in the flux of MAA across the sediment-water interface, due to much greater concentration gradients at the sediment-water interface resulting from a change in the balance between MAA production and consumption. This in turn led to decreased MAA concentrations and oxidation rates in surface sediments. These results suggest that the rapid consumption of MAA is important in retaining within the sediment the acetate produced by hydrolysis and fermentation of POC in the upper few cm of sediment.

The sensitivity of the models to the value chosen for the sediment diffusion coefficient was investigated by increasing D_s by factors of 10 and 100. This led to lower predicted concentrations in the upper few cm, while concentrations at depth were largely unaffected (Fig. 10b). Increasing D_s therefore enhanced diffusive loss of acetate across the sediment-water interface rather than increasing the acetate pool size deeper in the sediment. Accordingly, this led to decreased MAA turnover rates in the upper few cm of sediment rather than to an increase in MAA turnover rate at depth (Fig. 10e). Thus, even if random-type mixing processes associated with bioturbation or gas bubble ebullition were to enhance diffusive MAA transport in mid-Bay sediments, it would probably not increase MAA turnover rates at depth in the sediment.

The major differences between MAA concentration and turnover rate distributions predicted by the two models, along with the fact that consideration of diffusion did not alter predicted MAA distributions, lead us to reject the hypothesis that downward diffusion of acetate or other dissolved OC substrates produced by decay of MPOC in surface layers of mid-Bay sediments supports SR further down in the sediment. Because rates of acetate turnover in other coastal marine sediments are in general quite rapid and comparable to those found in the mid-Chesapeake Bay (Christensen and Blackburn, 1982; Shaw *et al.,* 1984; Novelli *et al.,* 1988; Michelson *et al.,* 1989), it is likely that our conclusions are valid for coastal sediments in general. The SR activity observed below ≈ 4 cm depth in mid-Bay and other coastal sediments must therefore be fueled by turnover of some portion of the large, relatively refractory pool of POC at depth in the sediment. This argument agrees with the results of Burdige (1991) which suggests that SR occurring at depth in southern

Chesapeake Bay sediments is fueled by material having a reactivity comparable to or perhaps even less than the G_2 material referred to by Westrich and Berner (1984).

In light of the above finding, it is reasonable to ask whether this more refractory POC, rather than new inputs of MPOC, could be important in fueling summer SR, which in total exceeds several-fold the amount of MPOC predicted to accumulate in mid-Bay surface sediments during the spring. Some simple calculations suggest that this is not the case. Two months of SR in mid-Bay sediments at average summer SR rates corresponds to oxidation of 5–6 mol C m^{-2}. If we assume a decay constant of ≈ 1 yr^{-1} (0.00274 d^{-1}) for the more refractory G_2 component of coastal sediment MPOC (Westrich and Berner, 1984; Brudige, 1991), then a pool size of at least $5/(60 \times 0.00274) \approx 30$ mol C m^{-2} would be required to supply this amount of SR. This quantity of POC is equal to 40–60% of the total POC pool in the upper 10 cm of R64 and DB sediments. Is this a realistic estimate of what the pool size of G_2 material could be in mid-Bay sediments? To evaluate this, let us assume that a steady-state balance exists between influx (J_{G2}) and degradation of G_2 material and that decay of this material occurs according to first-order kinetics with decay constant k, i.e.

$$dG_2/dt = J_{G2} - kG_2 = 0.$$

Let us also assume a constant rate of G_2 input and constant k value of 1 yr^{-1}. To estimate a value for J_{G2}, following Westrich and Berner (1984), we assume that 20% of total March–November weighted-average POC deposition to mid-Bay sediments (on the order of 100 mmol C m^{-2} d^{-1}) consists of G_2 material, i.e. let $J_{G2} = 20$ mmol C m^{-2} d^{-1}. The predicted steady-state pool size of G_2 material is then equal to $J_{G2}/k = (20/0.00274) = 7300$ mmol C m^{-2} (7.3 mol C m^{-2}). This value is only $\approx 25\%$ of the 30 mol C m^{-2} which would be required to fuel two months of SR in mid-Bay sediments. Although these calculations are crude, they indicate that G_2 material is not likely to be a major OC source for SR in mid-Bay sediments. Rather, as indicated above, this material probably fuels at most $\approx 1/3$ of total SR in the upper 12 cm of these sediments, mainly that occurring below 4 cm depth. Although it is possible that G_2 material fuels some SR in the upper 4 cm of sediment (particularly during the late summer when the MPOC (i.e., G_1) pools are likely at their seasonal minimum; Fig. 7), it appears that the degradation of G_1 material, continually resupplied by deposition from overlying waters, fuels the majority of SR occurring in mid-Bay sediments during the summer.

5. Summary and conclusions

Curve-fitting of dry weight POC distributions in mid-Chesapeake Bay sediments yielded MPOC pool size estimates of 2–3 mol C m^{-2}. Estimated MPOC concentrations decreased rapidly with depth in the sediment from 20–30% of total POC content at the surface to near zero at 10 cm depth. Integrated over the upper 10 cm, MPOC pools accounted for only $\approx 4\%$ of total POC. MPOC pool size estimates were

combined with sediment trap estimates of MPOC deposition to derive first-order decay constants for the decomposition of this material. The magnitude of these decay constant (≈ 10 yr^{-1}) suggested that this material is representative of the most readily degradable fraction of coastal marine phytoplankton detritus ("G_1" material; Westrich and Berner, 1984). Our estimates of the ratio of MPOC to total POC in surface sediments and of first-order MPOC decay constants are similar to those determined by curve-fitting in other organic rich coastal marine sediments (Martens and Klump, 1984). The fact that these parameters agree well with those determined experimentally in other coastal sediments (Westrich and Berner, 1984; Brudige, 1991) suggests that our procedures yielded reasonable estimates of the abundance and reactivity of G_1-type material in coastal sediments.

A simple kinetic model based on observed MPOC deposition rates and time/temperature-dependent first-order MPOC decay was used to predict seasonal (March–November) variations in MPOC pool size and turnover rate. The model predicted an accumulation of MPOC in sediments during the spring, followed by a decline during the summer. This pattern agrees with direct observations of seasonal variations of POC abundance in coastal marine sediments (Rudnick and Oviatt, 1986; Sampou and Oviatt, 1991). Maximum rates of MPOC turnover were predicted during the early summer, in agreement with early summer SR rate maxima observed in mid-Bay sediments. Predicted rates of MPOC turnover in the spring exceeded measured rates of SR. However, when sediment oxygen consumption-based estimates of spring aerobic carbon respiration are considered in addition to SR, the model predictions appear reasonable. Thus the simple model succeeded in describing both qualitatively and quantitatively the seasonal variation in mid-Bay sediment carbon metabolism, and the patterns predicted by the model are consistent with those described previously for other coastal marine sediments.

Steady-state and transient-state diagenetic models were used to evaluate the influence of particle mixing on mid-Bay sediment POC diagenesis. The results suggest that particle mixing distributes MPOC downward over the upper 4–6 cm of sediment, but that this process does not introduce MPOC to greater depths due to the rapid decay rate of this material. Steady-state models of acetate diagenesis were used to test the hypothesis that downward diffusion of microbially available acetate (MAA), produced by hydrolysis and fermentation of MPOC in the upper 4–6 cm of sediment, is important in fueling SR at greater depths in mid-Bay sediments. The results indicate that because of the low concentration (1–10 μmol L^{-1}) and rapid turnover rate (1–10 hr^{-1}) of MAA (both of which result from the high efficiency of SRB acetate uptake systems, which have a K_s of ≤ 5 μmol L^{-1} as determined from acetate uptake kinetics experiments in sulfate-reducing mid-Bay sediments), diffusion does not influence the depth distribution of acetate metabolism. Even at substantially elevated rates of MAA diffusion (100-fold higher than molecular diffusion), this process would not result in significant downward flux of MAA.

Therefore SR occurring at depths greater than 4–6 cm must be fueled by the turnover of some portion of the large, relatively refractory pool of POC. From the available data it was not possible to derive estimates of the pool size or decay constant for this less reactive POC pool, and therefore we did not attempt to incorporate a second (i.e. G_2) MPOC pool into the time-dependent kinetic model of POC turnover. This omission did not detract from the model's ability to accurately predict seasonal variations in sediment MPOC turnover, probably because such G_2-type material is likely to fuel only $\approx 1/3$ of total metabolism, i.e. carbon oxidation coupled to SR below 4 cm depth.

Taken together our results suggest that the kinetics of particulate and dissolved OC turnover in mid-Chesapeake Bay sediments are similar to those described for other coastal sediments, as are the temporal and spatial (down-core) patterns of carbon metabolism. However, an important distinction between mid-Bay and other coastal sediment metabolism is that with the onset of warm summer temperatures, the degradation of both stored and newly deposited MPOC is dominated by anaerobic microbial processes rather than by aerobic microbial respiration and/or transfer of this material upward through an aerobic benthic food chain.

APPENDIX

Abbreviations and notation

Chl-*a* Chlorophyll-*a*

D_m Random sediment particle mixing coefficient ($cm^2 \, yr^{-1}$)

D_s Sediment diffusion coefficient for MAA ($cm^2 \, d^{-1}$)

f Fraction of sediment SR fueled by MAA metabolism

G Dry weight sediment POC concentration ($mg \, C \, g^{-1}$)

G_o Dry weight sediment POC concentration at the sediment surface ($mg \, C \, g^{-1}$)

G_{nr} Dry weight "nonreactive" POC concentration at depth in the sediment ($mg \, C \, g^{-1}$)

G_m Dry weight sediment MPOC concentration ($mg \, C \, g^{-1}$)

G_m^o Dry weight MPOC concentration at the sediment surface ($mg \, C \, g^{-1}$)

G_m' Whole sediment MPOC concentration ($\mu mol \, C \, cm^{-3}$)

G_{ses} Dry weight POC concentration of suspended seston (mg C g^{-1})

G_1 The most labile fraction of MPOC in coastal marine phytoplankton (Westrich and Berner, 1984)

G_2 The less labile fraction of MPOC in coastal marine phytoplankton (Westrich and Berner, 1984)

J_{POC} Sediment POC deposition flux (μmol C cm^{-2} d^{-1} or mmol C m^{-2} d^{-1})

J_{MPOC} Sediment MPOC deposition flux (μmol C cm^{-2} d^{-1} or mmol C m^{-2} d^{-1})

k First-order MPOC decay constant (d^{-1} or yr^{-1})

k_{POC} First-order MPOC decay constant calculated from the ratio $J_{MPOC}{:}\Sigma G_m$ (d^{-1} or yr^{-1})

k_{SR} First-order MPOC decay constant calculated from the ratio $\Sigma SR{:}\Sigma G_m$ (d^{-1} or yr^{-1})

K Half-saturating pore water MAA concentration for acetate uptake in sediments (μM)

MAA Microbially Available Acetate

MPOC Metabolizable Particulate Organic Carbon

OC Organic Carbon

POC Particulate Organic Carbon

S_n Ambient MAA concentration in sediment pore waters (μM)

SR Sulfate Reduction

u MAA uptake rate constant (hr^{-1})

ω Sediment burial rate (cm yr^{-1})

ω_{dm} Mass sedimentation rate (g cm^{-2} yr^{-1})

ϕ Sediment porosity (volume fraction of water)

ΣG_m Depth-integrated pool of sediment of MPOC (μmol C cm^{-2})

ΣSR Depth-integrated summer sediment SR rate (μmol C cm^{-2} d^{-1} or mmol C m^{-2} d^{-1})

REFERENCES

Abdollahi, H., and D. B. Nedwell. 1979. Seasonal temperature as a factor influencing bacterial sulfate reduction in a salt marsh sediment. Microbiol. Ecol., 5, 73–79.

Ansbaek, J. and T. H. Blackburn. 1980. A method for the analysis of acetate turnover in a coastal marine sediment. Microbiol. Ecol., 5, 253–264.

Bågander, L. E. 1977. In situ studies of bacterial sulfate reduction at the sediment water interface. Ambio Special Report. 5, 147–155.

Balba, M. T. and D. B. Nedwell. 1982. Microbial metabolism of acetate, propionate, and butyrate in anoxic sediments from Colne Point saltmarsh, Essex, U.K. J. Gen Microbiol. 128, 1415–1422.

Banta, G. T., J. Tucker, A. E. Giblin and J. E. Hobbie. 1995. Benthic respiration and nitrogen release in Buzzards Bay, Massachusetts. J. Mar. Res., 53, 107–135.

Berner, R. A. 1964. An idealized model of dissolved sulfate distribution in recent sediments. Geochim. Cosmochim. Acta, 28, 1497–1503.

—— 1972. Sulfate reduction, pyrite formation, and the oceanic sulfur budget, *in* The Changing Chemistry of the Ocean, D. Dryssen and K. Jagner, K., eds., Almqvist and Wiksell, Stockholm, 347–361.

—— 1978. Sulfate reduction and the rate of deposition of marine sediments. Earth. Planet. Sci. Lett. *37,* 492–498.

—— 1980a. Early Diagenesis. Princeton University Press, Princeton.

—— 1980b. A rate model for organic matter decomposition in marine sediments, *in* Biogeochemistry of Organic Matter at the Sediment-Water Interface, 35–44, Comm. Natl. Recherche Scientifique (France) Reports.

Berner, R. A. and J. T. Westrich. 1985. Bioturbation and the early diagenesis of carbon and sulfur. Am. J. Sci., *285,* 193–206.

Boynton, W., W. M. Kemp, J. Garber, J. M. Barnes, L. L. Matteson, J. L. Watts, S. Stammerjohn, F. M. Rohland. 1900. Chesapeake Bay Water Quality Monitoring Program, Ecosystem Processes Component, Level 1 Report No. 7, Part 2: Data Tables. UMCEES Ref. No. 90-062CBL, Univ. of MD, Center for Environmental and Estuarine Studies, Chesapeake Biological Laboratory, Solomons, MD.

Burden, R. L., J. D. Faires and A. C. Reynolds. 1981. Numerical Analysis. Prindle, Weber, and Schmidt, Boston, 598 pp.

Burdige, D. J. 1991. The kinetics of organic matter mineralization in anoxic marine sediments. J. Mar. Res., *49,* 727–761.

Canfield, D. E. 1989. Sulfate reduction and oxic respiration in marine sediments: implications for organic carbon preservation in euxinic environments. Deep Sea Res., *36,* 121–138.

Capone, D. G. and R. P. Kiene. 1988. Comparison of microbial dynamics in freshwater and marine environments: contrasts in anaerobic carbon catabolism. Limnol. Oceanogr. *33,* 725–749.

Christensen, D. 1984. Determination of substrates oxidized by sulfate reduction in intact cores of marine sediments. Limnol. Oceanogr., *29,* 189–192.

Christensen, D. and T. H. Blackburn. 1982. Turnover of 14-C-labelled acetate in marine sediments. Appl. Environ. Microbiol., *31,* 227–233.

Dibb, J. E. and D. L. Rice. 1989. Temporal and spatial distribution of Beryllium-7 in the sediments of Chesapeake Bay. Estuar. Coast. Mar. Sci., *28,* 395–406.

Doering, P. H., C. A. Oviatt and J. R. Kelly. 1986. The effects of the filter feeding clam *Mercenaria mercenaria* on carbon cycling in experimental marine mesocosms. J. Mar. Res., *44,* 839–861.

Gibson, G. R., R. J. Parkes and R. A. Herbert. 1989. Biological availability and turnover rate of acetate in marine and estuarine sediments in relation to dissimilatory sulphate reduction. FEMS Microbiol. Ecol., *62,* 303–306.

Holland, A. F. 1988. Long-term variation of macrobenthos in a mesohaline region of Chesapeake Bay. Estuaries, *8,* 93–113.

Howarth, R. W. 1984. The ecological significance of sulfur in the energy dynamics of salt marsh and coastal marine sediments. Biogeochemistry. *1,* 5–27.

Jørgensen, B. B. 1977. The sulfur cycle of a coastal marine sediment (Limfjorden, Denmark). Limnol. Oceanogr., *28,* 814–822.

—— 1978a. A comparison of methods for the quantification of bacterial sulfate reduction in coastal marine sediments I. Measurement with radiotracer techniques. Geomicrobiol. J., *1,* 11–28.

—— 1978b. A comparison of methods for the quantification of bacterial sulfate reduction in

coastal marine sediments II. Calculations from mathematical models. Geomicrobiol. J., *1*, 11–28.

—— 1982. Mineralization of organic matter in the sea bed-the role of sulfate reduction. Nature, *296*, 643–645.

Kelly, J. R. and S. W. Nixon. 1984. Experimental studies of the effect of organic deposition on the metabolism of a coastal marine bottom community. Mar. Ecol. Prog. Ser., *17*, 157–169.

Kemp, W. M. 1988. An integrated view of ecological processes in mesohaline Chesapeake Bay: materials budget and simulation models. Trans. Am. Geophys. Union, *69*, 1096.

Kemp, W. M., P. Sampou, J. Caffrey, M. Mayer, K. Henriksen and W. R. Boynton. 1990. Ammonium recycling versus dentrification in Chesapeake Bay sediments. Limnol. Oceanogr., *35*, 1545–1563.

Kemp, W. M., P. Sampou, J. Garber, J. Tuttle and W. R. Boynton. 1992. Seasonal depletion of oxygen from bottom waters of Chesapeake Bay: roles of benthic and planktonic respiration and physical exchange processes. Mar. Ecol. Prog. Ser., *85*, 137–152.

Klump, J. V. and C. S. Martens. 1989. The seasonality of nutrient regeneration in an organic-rich coastal sediment: kinetic modeling of changing pore-water nutrient and sulfate distributions. Limnol. Oceanogr., *34*, 559–577.

Li, W. K. W. 1983. Consideration of errors in estimating kinetic parameters based on Michaelis-Menten formalism in microbial ecology. Limnol. Oceanogr., *28*, 185–190.

Lovley, D. R. and M. J. Klug. 1983. Sulfate reducers can outcompete methanogens at freshwater sulfate concentrations. Appl. Environ. Microbiol., *45*, 187–192.

Lovley, D. R. and E. J. P. Phillips. 1987. Competitive mechanisms for inhibition of sulfate reduction and methane production in the zone of ferric iron reduction in sediments. Appl. Environ. Microbiol., *53*, 2636–2641.

Mackin, J. E. and K. T. Swider. 1989. Organic matter decomposition pathways and oxygen consumption in coastal marine sediments. J. Mar. Res., *47*, 681–716.

Malone, T. C., L. H. Crocker, S. E. Pike and B. W. Wendler. 1988. Influences of river flow on the dynamics of phytoplankton production in a partially stratified estuary. Mar. Ecol. Prog. Ser., *48*, 235–249.

Malone, T. C., W. M. Kemp, H. W. Ducklow, W. R. Boynton, J. H. Tuttle and R. B. Jonas. 1986. Lateral variation in the production and fate of phytoplankton in a partially stratified estuary. Mar. Ecol. Prog. Ser., *32*, 149–160.

Martens, C. S. and J. V. Klump. 1984. Biogeochemical cycling in an organic-rich coastal marine basin 4. An organic carbon budget for sediments dominated by sulfate reduction and methanogenesis. Geochim. Cosmochim. Acta, *48*, 1987–2004.

Martin, W. R. and M. L. Bender. 1988. The variability of benthic fluxes and sedimentary remineralization rates in response to seasonally variable organic carbon rain rates in the deep sea: a modeling study. Am. J. Sci., *288*, 561–574.

Marvin, M. C. 1994. Controls on the spatial and temporal trends of benthic sulfate reduction and methanogenesis along the Chesapeake Bay central channel. Ph.D. Dissertation, University of Maryland, College Park, MD.

Matisoff, G. 1982. Mathematical models of bioturbation, *in* Animal-Sediment Relations, P. L. McCall and M. J. S. Tevesz, eds., Plenum Press, New York, 289–327.

Meyer-Reil, L. A. 1983. Benthic response to sedimentation events during autumn to spring at a shallow water station in the Western Kiel Bight. II. Analysis of benthic bacterial populations. Mar. Biol., *77*, 247–256.

Michelson, A. R., M. E. Jacobson, M. I. Scranton and J. E. Mackin. 1989. Modeling the distribution of acetate in anoxic estuarine sediments. Limnol. Oceanogr., *34*, 747–757.

Murray, J. W., V. Grundmanis and W. M. Smethie. 1978. Interstitial water chemistry in the sediments of Saanich Inlet. Geochim. Cosmochim. Acta, *42*, 1011–1026.

Novelli, P. C., A. R. Michelson, M. I. Scranton, G. T. Banta, J. E. Hobbie and R. W. Howarth. 1988. Hydrogen and acetate cycling in two sulfate-reducing sediments: Buzzards Bay and Town Cove, Mass. Geochim. Cosmochim. Acta., *52*, 2477–2486.

Officer, C. B., D. R. Lynch, G. H. Setlock and G. R. Helz. 1984. Recent sedimentation rates in Chesapeake Bay, *in* The Estuary as a Filter, V. S. Kennedy, ed., Academic Press, New York, 131–158.

Parkes, R. J., G. R. Gibson, I. Mueller-Harvey, W. J. Buckingham and R. A. Herbert. 1989. Determination of the substrates for sulphate-reducing bacteria within marine and estuarine sediments with different rates of sulphate reduction. J. Gen. Microbiol., *135*, 175–187.

Parkes, R. J., J. Taylor and D. Jørck-Ramberg. 1984. Demonstration, using *Desulfobacter* sp., of two pools of acetate with different biological availabilities in marine pore water. Mar. Biol., *83*, 271–276.

Peng, T. H. and W. S. Broecker. 1979. Rates of benthic mixing in deep-sea sediment as determined by radioactive tracers. Quat. Res., *11*, 141–149.

Press, W. H., S. A. Teukolsky, W. T. Vetterling and B. P. Flannery. 1992. Numerical Recipes, 2nd Edition. Cambridge University Press, Cambridge.

Reeburgh, W. S. 1969. Observations of gases in Chesapeake Bay sediments. Limnol. Oceanogr., *14*, 368–375.

Roden, E. E. and J. H. Tuttle. 1992. Sulfide release from estuarine sediments underlying anoxic bottom water. Limnol. Oceanogr., *37*, 725–737.

—— 1993. Inorganic sulfur cycling in mid and lower Chesapeake Bay sediments. Mar. Ecol. Prog. Ser., *93*, 101–118.

Roden, E. E., J. H. Tuttle, W. R. Boynton and W. M. Kemp. 1995. Carbon cycling in mesohaline Chesapeake Bay sediments 1. POC deposition and mineralization pathways. J. Mar. Res., *53*, 799–819.

Rudnick, D. T. and C. A. Oviatt. 1986. Seasonal lags between organic carbon deposition and mineralization in marine sediments. J. Mar. Res., *44*, 815–837.

Sampou, P. and C. A. Oviatt. 1991. Seasonal patterns of sedimentary carbon and anaerobic respiration along a simulated eutrophication gradient. Mar. Ecol. Prog. Ser., *72*, 271–282.

Sansone, F. J. and C. S. Martens. 1982. Volatile fatty acid cycling in organic-rich marine sediments. Geochim. Cosmochim. Acta., *46*, 1575–1589.

Sellner, K. G. 1987. Phytoplankton in Chesapeake Bay: role in carbon, oxygen, and nutrient dynamics, *in* Contaminant Problems and Management of Living Chesapeake Bay Resources, S. K. Majumdar, L. W. Hall and M. A. Herbert, eds., Pennsylvania Academy of Sciences, Phillipsburg, 134–157.

Shaw, D. G., M. J. Alperin, W. S. Reeburgh and D. J. McIntosh. 1984. Biogeochemistry of acetate in anoxic sediments of Skan Bay, Alaska. Geochim. Cosmoschim. Acta, *48*, 1819–1825.

Shaw, D. G. and D. J. McIntosh. 1990. Acetate in recent anoxic sediments: direct and indirect measurements of concentrations and turnover rates. Estuar. Coast. Shelf Sci., *31*, 775–788.

Sørensen, J., D. Christensen and B. B. Jørgensen. 1981. Volatile fatty acids and hydrogen as substrates for sulfate reducing bacteria in anaerobic marine sediment. Appl. Environ. Microbiol., *42*, 5–11.

Sun, M., R. C. Aller and C. Lee. 1991. Early diagenesis of chlorophyll-*a* in Long Island Sound sediments: a measure of carbon flux and particle reworking. J. Mar. Res., *49*, 379–401.

Toth, D. J. and A. Lerman. 1977. Organic matter reactivity and sedimentation rates in the ocean. Am. J. Sci., *277*, 265–285.

Turekian, K. K., G. J. Benoit and L. K. Benninger. 1980. The mean residence time of plankton derived carbon in a Long Island Sound sediment core: A correction. Estuar. Coast. Mar. Sci., *11*, 583–587.

Tuttle, J., R. Jonas and T. Malone. 1987. Origin, development and significance of Chesapeake Bay anoxia, *in* Contaminant Problems and Management of Living Chesapeake Bay Resources, S. K. Majumdar, L. W. Hall Jr., and M. A. Herbert, eds., Pennsylvania Academy of Sciences, Phillipsburg, 442–472.

Wellsbury, P. and R. J. Parkes. 1995. Acetate bioavailability and turnover in an estuarine sediment. FEMS Microb. Ecol., *17*, 85–94.

Westrich, J. T., and R. A. Berner. 1984. The role of sedimentary organic matter in bacterial sulfate reduction: The G model tested. Limnol. Oceanogr., *29*, 236–249.

—— 1988. The effect of temperature on rates of sulfate reduction in marine sediments. Geomicrobiol. J., *6*, 99–117.

Winfrey, M. R. and D. M. Ward. 1983. Substrates for sulfate reduction and methane production in intertidal sediments. Appl. Environ. Microbiol., *45*, 193–199.